A&A 412, 57–67 (2003)
DOI: 10.1051/0004-6361:20031412

Astronomy & Astrophysics

HYPERLEDA

II. The homogenized HI data⋆

G. Paturel[1], G. Theureau[2,3], L. Bottinelli[2,4], L. Gouguenheim[2,4], N. Coudreau-Durand[2], N. Hallet[2], and C. Petit[1]

[1] Observatoire de Lyon, avenue Charles-André, 69561 Saint-Genis Laval Cedex, France
[2] LPCE, CNRS-Orléans, 3A avenue de la recherche scientifique, 45071 Orléans Cedex 02, France
[3] Observatoire de Paris-Meudon, GEPI, 5 place Jules Janssen, 92195 Meudon Cedex, France
[4] Université Paris-Sud, Bât. 470, 15 rue Georges Clémenceau, 91405 Orsay Cedex, France

Received 25 March 2003 / Accepted 29 July 2003

Abstract. After a compilation of HI data from 611 references and new observations made in Nançay, we produce a catalog of homogenized HI data for 16781 galaxies. The homogenization is made using the EPIDEMIC method from which all data are progressively converted into the adopted standard. The result is a catalog giving: 1) the logarithm of twice the maximum rotation velocity, $\log 2V_{\rm M}^{\sin i}$, converted to the system of Mathewson et al. (1996). This quantity is given without correction for inclination; 2) the HI magnitude, m_{21}, (area of the 21-cm line width expressed in magnitude) converted to the flux system of Theureau et al. (1998); 3) the HI velocity, $V_{\rm HI}$, expressed with the optical definition (i.e., using wavelengths instead frequencies). The typical uncertainties are: 0.04 for $\log 2V_{\rm M}^{\sin i}$, 0.25 mag for m_{21} and 9 km s^{-1} for $V_{\rm HI}$.

Key words. galaxies: general – catalogs

1. Introduction

Our first compilation of HI-data (Bottinelli et al. 1982) associated with optical ones was the origin of the LEDA database. The specificity of LEDA is to provide mean homogenized parameters, in the spirit of the series of Reference Catalogues initiated by G. and A. de Vaucouleurs (see the RC3 by de Vaucouleurs et al. 1991). The Tully-Fisher relation (Tully & Fisher 1977) is the most straightforward application of such a large collection of HI and optical measurements.

The data are regularly maintained and the methods of homogenization are regularly revisited in order to take into account the evolution of measurements. In 1982 we collected HI measurements (21-cm line width, HI flux or HI radial velocity) for 1210 galaxies (Bottinelli et al. 1982) and for 6439 galaxies in 1990 (Bottinelli et al. 1990). Today, we have measurements for 16 781 galaxies. This increase could alone justify a new publication but another reason pushes us to revisit the method of homogenization: Many new measurements of logarithms of rotation velocity (hereafter, $\log 2V_{\rm M}^{\sin i}$), obtained from rotation curves, are now available in the literature. This gives us a new way to convert directly the observed 21-cm line widths into the astrophysical parameter $\log 2V_{\rm M}^{\sin i}$.

Further, the velocity resolution has been considerably improved (in 1982, 32 percent of our catalogue had measurements with a poor resolution of 63.5 km s^{-1} and only 50 percent of the sample were obtained with a resolution better than 25 km s^{-1}. In the present catalogue, 92 percent of the data are obtained with a resolution better than 25 km s^{-1} and only a few galaxies (46) have no resolution better than 50 km s^{-1}. This means that the correction for instrumental effects can be made effectively using a simple linear approximation.

In Sect. 2 we give a description of the present compilation of HI data in which new observations are included. The new observations are presented in the appendix. In Sect. 3 we briefly review the method of analysis (the EPIDEMIC method) applied to this study. Then, in Sects. 4–6, we study the homogenization of 21-cm line widths, of HI radial velocities and of 21-cm line fluxes, respectively. This allows us to produce a catalog of mean homogenized HI data, presented in the final section.

These data, together with the whole catalogue, are now available through the HYPERLEDA database (`leda.univ-lyon1.fr`), a project which aims at extending the capabilities of LEDA.

2. Main characteristics of the HI-compilation

We collected HI data from 611 papers. The full references with their code numbers are available in electronic form at the CDS.

Send offprint requests to: G. Paturel,
e-mail: `patu@obs.univ-lyon1.fr`

⋆ Full Tables 4, 5, 6, 7 and Fig. A.1 are available in electronic form at `http://www.edpsciences.org`.
Full Tables 3, 8, A.1 and A.3 are available in electronic form at the CDS via anonymous ftp to
`cdsarc.u-strasbg.fr (130.79.128.5)` or via
`http://cdsweb.u-strasbg.fr/cgi-bin/qcat?J/A+A/412/57`

Table 1. List of telescopes. Column 1: number of published 21-cm line widths; Col. 2: code number of the telescope in LEDA; Col. 3: Name of the telescope.

n	code	Radiotelescope
19 291	9	Arecibo
10 089	1	Nançay
8702	7	NRAO (91 m)
3209	10	Parkes
2476	8	Effelsberg
1245	3	NRAO (43 m)
1062	5	Jodrell B. (MarkI)
816	2	Westerbork
244	14	Jodrell B. (MarkII)
114	11	Owens Valley
451	15	VLA
86	6	Harvard
54	12	Dwingeloo
38	4	Cambridge
37	13	IAR (Argentina)
3199		Optical
51 113		total

Further, for 809 galaxies we added new measurements made with the radiotelescope of Nançay. These new data are presented in the appendix.

This compilation provides us with 51 113 measurements of 21-cm line widths or maximum velocity rotation, 31 157 measurements of HI radial velocity and 25 764 measurements of HI flux (area of the 21-cm line) for 16 781 galaxies. These data are characterized by some secondary parameters: telescope, velocity resolution, definition of the 21-cm line width and bibliographic reference. Some additional parameters are also required: For instance the diameter and axis ratio of the observed galaxy (and sometimes the position angle) are needed to correct for the beam filling effect (see the section where the homogenization of fluxes is described). The optical radial velocity is also useful to provide a final check of velocities. These additional parameters are taken from LEDA.

Table 1 gives the list of telescopes with their code number and the number of 21-cm line widths obtained by each.

Figure 1 gives the histogram of velocity resolutions. These resolutions will be shared in four classes designated by r, where r represents the mean velocity resolution in km s^{-1} (see Table 4):

- $resol. \leq 10$ km s^{-1} ($r = 8$ km s^{-1});
- 10 km s^{-1} $< resol. \leq 18$ km s^{-1} ($r = 16$ km s^{-1});
- 18 km s^{-1} $< resol. \leq 25$ km s^{-1} ($r = 21$ km s^{-1});
- 25 km s^{-1} $< resol.$ ($r = 41$ km s^{-1}).

When the measurements are entered in our database, each 21-cm line width receives a code defining how the measurement was done. These codes are given in Table 2 with their definitions and the number of occurences.

Finally, Table 3 presents the references giving more than 300 measurements. The reference numbers are arbitrary. They are internal numbers in LEDA. The full table, sorted by the number of entries, is available in electronic form at the CDS. It is also available sorted in alphabetic order.

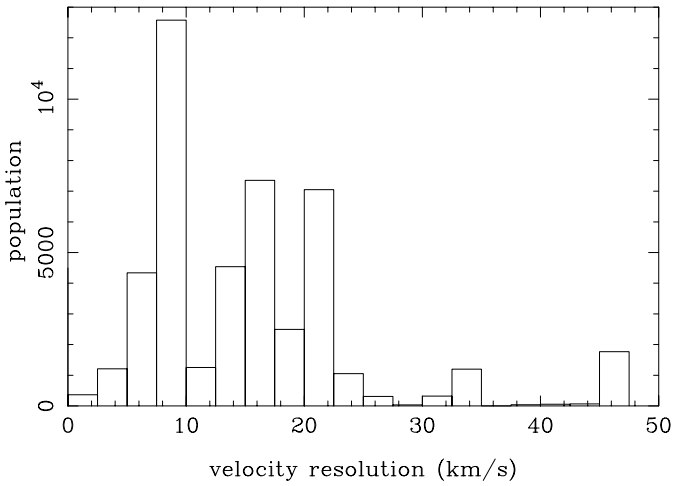

Fig. 1. Histogram of velocity resolutions.

Table 2. Definition of the method of measurement of 21-cm line width. The columns are arranged as follows: Col. 1: number of published 21-cm line widths; Col. 2: code number of the method in LEDA; Col. 3: description of the method.

n	code	Definition of the level
20 684	5	50% of the maximum
17 546	1	20% of the maximum
4702	8	50% of the mean
3067	10	$2V_{\rm M}^{\sin i}$ from rotation curve
1503	4	40% of the maximum
1268	2	25% of the maximum
1069	6	20% of the mean
731	9	mean of codes 1 and 8
395	7	25% of the mean
139	0	undetermined
51 113		total

3. Description of the analysis: The EPIDEMIC method

At the time of the construction of our previous catalogs there was no standard system for 21-cm measurements. This obliged us to refer the measurements to a mean system using the INTERCOMP method (see, Bottinelli et al. 1982). Today, thanks to some large homogeneous samples, it is possible to convert the measurements directly. This leads us to use a new method of analysis, the EPIDEMIC method (Paturel et al. 2003, Paper I). We start from a standard sample (a set of measurements giving a large and homogeneous sample). All other measurements are grouped into homogeneous classes (for instance, the class of measurements made at a given level and obtained with a given velocity resolution). Each class is cross-identified with the standard sample in order to establish the equation of conversion to the standard system. Then, the whole class is included in the standard sample which grows progressively (epidemic propagation). The order of inclusion follows the inverse of the quantity $t = \sigma/\sqrt{n}$, where σ is the

Table 3. List of the richest references ($n > 300$). The columns are arranged as follows: Col. 1: number of measurements of 21-cm line width or $\log 2V_{\rm M}^{\sin i}$; Col. 2: code number of the reference in LEDA; Col. 3: Full reference. The full table is available in electronic form at the CDS.

N	code	Reference
4152	23289	Theureau G., Bottinelli L., Coudreau-Durand N., et al. 1998, AAS, 130,333
2258	18000	Fisher J. R., & Tully R. B. 1981, ApJS, 47, 139
2048	23286	Mathewson D. S., & Ford V. L. 1996, ApJS, 107, 97
1392	23359	(this paper)
1361	23225	Giovanelli R., Haynes M. P. 1993, AJ, 105(4), 1271
1267	16120	Bottinelli L., Gouguenheim L., & Paturel G. 1982, AA, 113, 61
1166	23296	Giovanelli R., Avera E., & Karachentsev I. D. 1997, AJ, 114(1), 122
1048	23200	Schneider S. E., Thuan T. X., Mangum J. G., et al. 1992, ApJS, 81, 5
1036	24372	Haynes M. P., Giovanelli R., Chamaraux P., Da Costa L. N., et al. 1999, AJ, 117, 2039
854	23151	Giovanelli R., & Haynes M. P. 1989, AJ, 97, 633
757	23122	Haynes M. P., Giovanelli R., Starosta B. M., et al. 1988, AJ, 95, 607
726	23087	Lewis B. M., Helou G., Salpeter E. E. 1985, ApJS, 59, 161
691	23070	Giovanelli R., & Haynes M. P. 1985, AJ, 90, 2445
636	23117	Lewis B. M. 1987, ApJS, 515-542
628	23123	Tifft W. G., & Cocke W. J. 1988, ApJS, 67, 1-75
610	23152	Giovanelli R., Haynes M. P., Myers S. T., & Roth J. 1986, AJ, 92, 250
602	23192	Haynes M. P., & Giovanelli R. 1991, ApJS, 77, 331
546	16117	Thuan T. X., & Seitzer P. O. 1979, ApJ, 231, 327
535	23224	Wegner G., Haynes M. P., & Giovanelli R. 1993, AJ, 105(4), 1251
513	23092	Bicay M. D., & Giovanelli R. 1986, AJ, 91, 732
496	23091	Bicay M. D., & Giovanelli R. 1986, AJ, 91, 705
485	23226	Lu N. Y., Hoffman G. L., Groff T., et al. 1993, ApJS, 88,383
482	23195	Fouque P., Bottinelli L., Durand N., et al. 1990, AAS, 86, 473
481	23172	Richter O. G., & Huchtmeier W. K. 1991, AAS, 87, 425
474	23444	Rosenberg J. L., & Schneider S. E. 2000, ApJS, 130, 177
474	16093	Shostak G. S. 1978, AA, 68, 321
472	23351	Impey C. D., Burkholder V., & Sprayberry D. 2001, AJ, 122, 2341
472	23067	Bothun G. D., Aaronson M., Schommer R. A., et al. 1985, ApJS, 57, 423
448	23335	Matthews L. D., & van Driel W. 2000, AAS, 143, 421
439	23284	Haynes M. P., Giovanelli R., Herter T., et al. 1997, AJ, 113(4), 1197
436	23333	Huchtmeier W. K., Karachentsev I. D., Karachentseva V. E., et al. 2000, AAS, 141, 469
427	16057	Rubin V. C., Ford Jr. W. K., Thonnard N., et al. 1976, AJ, 81, 687
423	16081	Dickel J. R., & Rood H. J. 1978, ApJ, 223, 391
367	12158	Peterson S. D. 1979, ApJS, 40, 527
345	23113	Hoffman G. L., Helou G., & Salpeter E. E., et al. 1987, ApJS, 63, 247
344	23269	Lu N. Y., & Freudling W. 1995, ApJ, 449, 527
312	23121	Staveley-Smith L., & Davies R. D. 1988, MN, 231, 833-871
...	...	...
...	...	...
...	...	...

standard deviation of a preliminary comparison and n the number of measurements. References having no intersection with the standard sample during the preliminary comparison are included following their population. All inclusions are made using weighted means. The standard sample receives the best standard deviation divided by $\sqrt{2}$. This assumes that it has the same scatter as the second best sample.

Obviously, the parameters used to make the classification must be relevant and we have to check that the equation of conversion is properly defined. Further, it is necessary to check that the conversion equation is reasonable (for instance, the conversion of flux should have a slope not very different from one in a log–log scale). Let us see now the application of this method to the homogenization of rotation velocities, heliocentric radial velocities and HI fluxes.

4. Homogenization of rotation velocities

4.1. First step

The 21-cm line widths are used to derive the maximum rotation velocity $V_{\rm M}^{\sin i}$. It is important to note that in this paper, we consider always the quantity $\log 2V_{\rm M}^{\sin i}$, that is twice the maximum rotation velocity in a logarithmic scale, in order to have a definition comparable with the log of a 21-cm line width. Note that $\log 2V_{\rm M}^{\sin i}$ is not corrected for the inclination.

The physical parameter measuring the maximum velocity rotation V_M is then related to $\log 2V_M^{\sin i}$ following the relation

$$\log V_M = \log 2V_M^{\sin i} - \log 2 \sin i \quad (1)$$

where i is the inclination of the galaxy (angle between the line of sight and the polar axis of the galaxy). Note that this relation implies a symmetric rotation curve. For non interacting galaxies this is reasonably justified.

The raw 21-cm line widths are denoted $\log W$. They must be corrected for instrumental effects (velocity resolution r, standardization of the level of measurement, l) and then converted into $\log 2V_M^{\sin i}$ after correcting for internal velocity dispersion.

The adopted standard sample of $\log 2V_M^{\sin i}$ deduced from rotation curves is the sample by Mathewson et al. (1996) because it is the largest homogeneous one. Our new way of analysis allows us to convert directly $\log W(r,l)$ into $\log 2V_M^{\sin i}$ because we now have a large enough standard sample of $\log 2V_M^{\sin i}$. The correction for the resolution, the conversion to a standard level of measurement and the correction of internal dispersion are all done in a single operation provided that the data are distributed into homogeneous subsamples.

The choice of a log–log conversion relation can be predicted in the case of good velocity resolution. However, we verified that it is linear. As an example, we show in Fig. 2 the relationship for the two richest subsamples.

It can be noted that some discrepant points are visible. They can result from an HI confusion by a close galaxy present in the lobe of the radiotelescope or from a bad detection. These discrepant objects are recorded for each regression in order to put a question mark on the final $\log 2V_M^{\sin i}$ value.

The total sample is divided into 26 subsamples defined by a given resolution r and a given level l. After the preliminary test, the standard deviation of the initial standard sample of $\log 2V_M^{\sin i}$ is taken as $\sigma(\log 2V_M^{\sin i}) = 0.027$. The results of the EPIDEMIC method is shown in Table 4. This table gives the slope a and the intercept b of the equation:

$$\log 2V_M^{\sin i} = a.\log W(r,l) + b. \quad (2)$$

It also gives the standard deviation σ, the number of points n of the regression, and N_s, the growing number of standard measurements.

This table gives the coefficients to convert any 21-cm line width (measured with a resolution r at a level l) into $\log 2V_M^{\sin i}$. It gives also the standard deviation σ assigning a weight $1/\sigma^2$ to the measurement.

It is visible from Table 4 that the level $l = 5$ (50% of the maximum) gives a slope close to one, while the level $l = 1$ (20% of the maximum) gives a slope significantly larger. One can see also that the low-resolution class ($r = 41$ km s^{-1}), for $l = 1$ or $l = 5$, gives systematically larger standard deviations. This reflects the fact that this class is less accurate and less homogeneous.

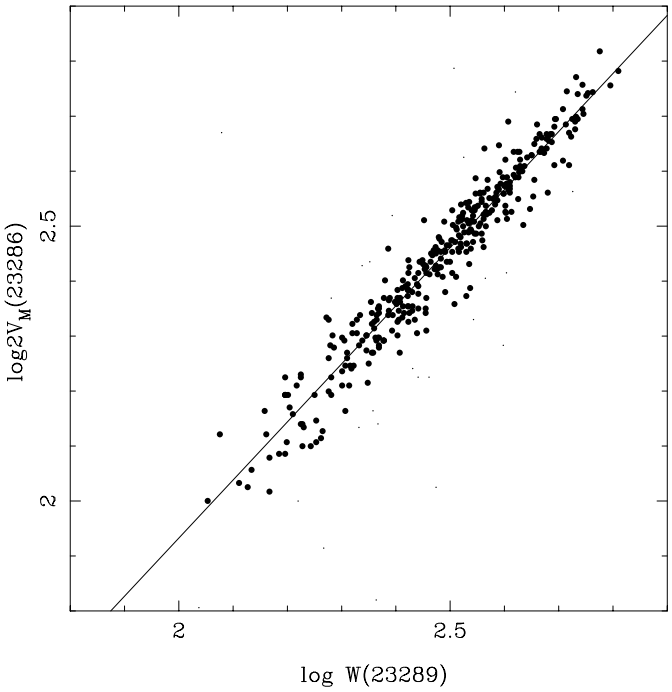

Fig. 2. An example of the regression used to convert log of 21-cm line widths $\log W(r,l)$ into $\log 2V_M^{\sin i}$. Both quantities are observed ones, uncorrected for inclination. $\log W(r,l)$ refers to measurements made with a same class of velocity resolution and a same level of measurement. The regression is quite linear. The list of discrepant measurements (tiny dots) obtained with all references will be used to correct (or to erase) doubtful measurements.

Table 4. Correction of $\log W(r,l)$ to $\log 2V_M^{\sin i}$. This table gives the conversion coefficients and the mean error for the 26 subsamples (level and resolution). l is the level code (see Table 2). r is the mean velocity resolution in km s^{-1}. The full table is available in the electronic version of the journal.

l	r	$a \pm \sigma_a$	$b \pm \sigma_b$	σ	n	N_s
5	8	1.071 ± 0.009	-0.210 ± 0.023	0.044	928	2933
1	8	1.187 ± 0.002	-0.543 ± 0.005	0.036	5309	8952
1	21	1.193 ± 0.005	-0.563 ± 0.012	0.043	1438	9371
		...	...			
		...	...			
		...	...			

4.2. Test reference by reference

As a refinement[1] we apply again the EPIDEMIC method using the bibliographic references to define the different homogeneous classes. The $\log 2V_M^{\sin i}$ measurements by Mathewson et al. (1996) are used as a standard. For this application, the $\log W(r,l)$ are first converted to $\log 2V_M^{\sin i}$ using the previous result (Table 4). This will allow us to improve the results for some references. If the first correction was perfect, the new

[1] We search also for the effect of beam filling on $\log 2V_M^{\sin i}$. We found a very tiny effect $\delta(\log 2V_M^{\sin i}) = (0.0028 \pm 0.0013)\theta - (0.0024 \pm 0.0011)$, ($\theta$ is the angular resolution of the radiotelescope, as seen in Sect. 5) that had no practical effect on the final result. Further, this effect disappeared for large galaxies ($\log D_{25} > 1.5$) where it is supposed to be more significant. We thus decided, for simplicity, to neglect it.

Table 5. Correction of $\log 2V_{\rm M}^{\sin i}$ to the adopted standard (ref. 23286). This table gives the conversion coefficients and the mean error for the 65 references requiring an additional correction. The full table is available in the electronic version of the journal.

Ref.	$a \pm \sigma_a$	$b \pm \sigma_b$	σ	n	$N_{\rm s}$
23289	1.000 ± 0.000	−0.007 ± 0.002	0.036	390	2439
18000	1.054 ± 0.010	−0.132 ± 0.024	0.024	158	4084
23121	1.026 ± 0.010	−0.058 ± 0.024	0.021	95	5064
...	...	...			
...	...	...			
...	...	...			

slope should be $a = 1$ and the zero-point should be $b = 0$ for any references. We keep only those references for which the slope or the zero point are significantly different from that. A Student's t-test is first made on the slope a. If the slope is not significantly different from 1 at the 0.01 probability level, it is taken as 1, exactly, and b is recalculated. Another t-test is made on the new b value. If it does not differ significantly from zero the reference does not need additional correction. Otherwise, the values of a or b are adopted, as given in Table 5. 65 references needed an additional correction. We established a list of 2087 galaxies that may have one discrepant measurement. This list will be used when we construct the final homogeneous catalog.

5. Homogenization of HI fluxes

5.1. Preliminary correction

The raw fluxes F collected in the literature are converted into a logarithmic scale using m_{21} magnitudes defined as (Vaucouleurs et al. 1991):

$$m_{21} = -2.5 \log(0.2366F) + 15.84 \quad (3)$$

F in Jy km s^{-1}

Before applying the EPIDEMIC method, these magnitudes must be corrected for the beam filling effect. Sometimes radioastronomers publish corrected fluxes but, when possible, we prefer to collect raw fluxes in order to have a homogeneous conversion. The form of the correction is well established. We will use the correction established in our previous study (Bottinelli et al. 1990). Let us recall how the corrected HI magnitude, m_{21}^c, is calculated:

$$m_{21}^c = m_{21} - 1.25 \log[(1 + xT)(1 + xt)] \quad (4)$$

$$T = D_{25}^2/\theta^2 \quad (5)$$

$$t = d_{25}^2/\theta^2 \quad (6)$$

D_{25} and d_{25} are respectively the major and minor axis diameter at the 25 $B-$mag arcsec^{-2} and θ is the half power beam size of the considered radiotelescope. In this equation D_{25}, d_{25} and θ are expressed with the same unit (i.e. arcmin). The parameter x is $x = 0.72 \pm 0.06$ (Bottinelli et al. 1990). We will keep this value.

Table 6. Correction of m_{21} to the scale of Nançay. This table gives the the zero-point shift and the mean error for the different radiotelescope (Col. 1). By its adoption as a standard, the Nançay radiotelescope ($t = 1$) has $b = 0$ and its standard deviation is $\sigma = 0.24$. The full table is available in the electronic version of the journal.

t	$b \pm \sigma_b$	σ	n	$N_{\rm s}$
7	0.052 ± 0.016	0.393	647	4182
9	−0.086 ± 0.013	0.415	1043	6413
3	0.051 ± 0.012	0.260	467	12813
	...	...		
	...	...		
	...	...		

For the Nançay radiotelescope the correction is more complex because the half power beam is not circular ($\approx 21'$NS $\times$ $4'$EW). We adopted the the same correction (Rel. (4)) but:

$$T = (D_{25}^2 \sin^2\beta + d_{25}^2 \cos^2\beta)/\theta_{\rm EW}^2 \quad (7)$$

$$t = (D_{25}^2 \cos^2\beta + d_{25}^2 \sin^2\beta)/\theta_{\rm NS}^2 \quad (8)$$

where β is the position angle of the considered galaxy (counted from North towards East) and where the ellipse of the half power bean size is defined by $\theta_{\rm EW} = 4'$ and $\theta_{\rm NS} = 21'$. D_{25}, d_{25} and β are calculated following Paturel et al. (2003, Paper I).

5.2. Homogenization by telescope

The EPIDEMIC method can now be applied to m_{21}^c. We expect a systematic effect depending on the radiotelescope itself. Thus, the classification of the EPIDEMIC method is built using the code for each radiotelescope. We use the Nançay radiotelescope ($t = 1$) as a standard because its large beam is less sensitive to the beam filling effect and because it constitutes one of the largest sample (see Table 1). The adopted equation of conversion is:

$$m_{21}^c(t = 1) = m_{21}^c(t) + b. \quad (9)$$

This equation assumes that there is no significant scale error but only a zero-point shift. This is what we assumed in our previous HI catalogs, in agreement with the result (Paturel et al. 1991) that apparent differences in scale often reflect different limiting magnitudes. The result for each radiotelescope is given in Table 6.

5.3. homogneization reference by reference

We check reference by reference to find specific corrections of the zero-point of the m_{21}^c magnitudes. They are first converted to the Nançay scale using the results from Table 6. For this second run, we adopted as a standard the reference 23289. Nevertheless, in order to reduce the number of references requiring a specific correction, it has been shifted by 0.2 mag (this correction has been obtained from a weighted mean of individual shifts, reference by reference). In other words,

Table 7. Correction of m_{21} to the standard (ref. 23289). This table gives the zero-point shift and its mean error for the 46 references requiring an additional correction. The full table is available in the electronic version of the journal.

Ref.	$b_r \pm \sigma_{b_r}$	σ	n	N_s
23195	-0.177 ± 0.019	0.147	61	2997
23321	-0.134 ± 0.031	0.183	41	3625
23359	-0.095 ± 0.036	0.266	56	3866
...	...	...		
...	...	...		
...	...	...		

the actual zero-point of the magnitude scale is built from a mean system. The final m_{21}^F magnitudes is then given by:

$$m_{21}^F = m_{21}^c(t = 1) + b_r - 0.2. \quad (10)$$

The value of b_r is zero except for 46 references for which it is given in Table 7.

6. Homogenization of HI radial velocities

The EPIDEMIC method is now used for the heliocentric radial velocities. Note that all these velocities should be expressed with the optical convention $V = c(\lambda - \lambda_\circ)/\lambda_\circ$. We do not expect any sources of systematic effects. Thus we simply check that there is no reference effect. The homogeneous classes of the EPIDEMIC method are thus made using the reference code. The standard sample is the reference 23289 because it is the largest one. Two references (23000 and 23316) show a significant effect. It appears that they are expressed as $V = c(\nu_\circ - \nu)/\nu_\circ$, where ν is the frequency. This effect disappears for these references when we applied the correction $V = V(\nu)/(1 - V(\nu)/c)$. One reference (23286) showed a barely significant departure from the standard. It could have been corrected by applying a scaling factor $V_{\rm corr.} = (1.0016 \pm 0.0008)V$. Because reference 23286 was adopted as the standard for rotation velocity measured from rotation curves, one can ask if this effect could affect the accuracy of $\log 2V_{\rm M}^{\sin i}$. One can calculate that this effect is at least 40 times smaller than the typical uncertainty and is completely negligible.

Finally, we have to estimate the standard deviation for each reference. As we did in our previous compilations, the best way consists of finding a correlation between the standard deviation and the resolution velocity. For this purpose, we apply the EPIDEMIC method using the true velocity resolution R as a parameter of classification. For each regression we get the standard deviation and we plot it as a function of the resolution. The result is shown in Fig. 3. A direct regression leads to the relation: $\sigma = 0.2R + 6$. This result is compatible with the result we obtained earlier (Bottinelli et al. 1990): $\sigma = 0.15R + 7.4$. Nevertheless, we prefer to calculate the regression using only the resolution smaller than 24 km s^{-1} because the sample is dominated by small resolutions (see Fig. 1). The result is thus

$$\sigma = (0.30 \pm 0.10).R + (5.5 \pm 1.4). \quad (11)$$

This leads to increased σ for large resolutions, i.e., to reduce the weight of old, poor resolution measurements. This justifies also that we adopted this last solution. In Fig. 3 this solution is drawn.

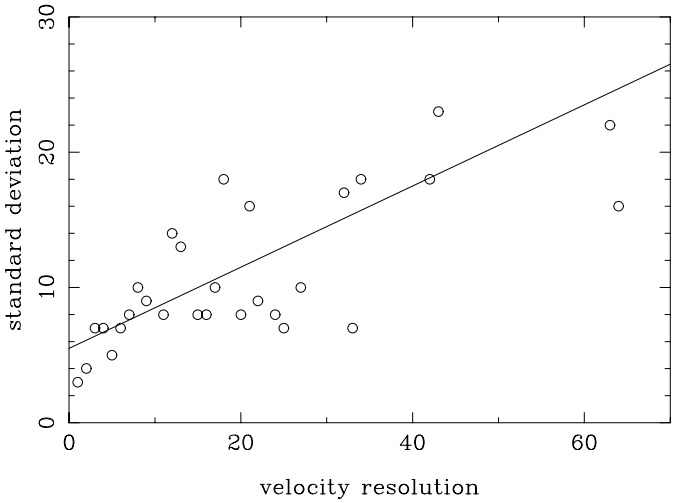

Fig. 3. Empirical relation between the velocity resolution r and the standard deviation σ of the regressions $V(r)$ vs. $V(\text{ref} = 23289)$. The adopted solution calculated with the resolution smaller than 24 km s^{-1} is represented by the full line.

We established a list of 710 galaxies that may have one discrepant velocity to be noted in the final homogeneous catalog.

As an additional test, we checked the homogenized HI velocities against the optical ones extracted from the LEDA database. The direct regression leads to the following result (obtained with 10 019 galaxies):

$$V(optical) = (1.0000 \pm 0.001).V_{\rm HI} - (5.3 \pm 0.7). \quad (12)$$

Stricto Sensu, the zero-point is significantly different from 0. However, the standard deviation is $\sigma = 39$ km s^{-1} and the mean difference of both systems ($\Delta V = 5.3$ km s^{-1}) has no practical incidence. This comparison provided us with another list of 634 galaxies for which there is a discrepancy between optical and HI velocities.

7. The final catalogue of homogenized HI data

Using the results of the previous sections we produced a catalog of homogenized HI data for 16 781 galaxies. The distribution of heliocentric radial velocities (Fig. 4) shows a bump around 5000 km s^{-1}, although the completeness in volume is satisfied only up to ≈2000 km s^{-1}. This corresponds to the nearest clusters surrounding the Local Super Cluster.

Let us recall briefly how the homogenized data are calculated. The 21-cm line widths are first converted into $\log 2V_{\rm M}^{\sin i}$ using empirical linear relations (Table 4) depending on the velocity resolution and on the level of measurement. For some references an additional correction is applied (Table 5). The mean error of each individual measurement comes from the standard deviation of the linear regression used for the last conversion (Tables 4 or 5). The HI magnitudes $m21$ are first corrected for the beam filling effect (Rel. (4)) and then converted to the Nançay scale using linear relations (Table 6) depending on the radiotelescope used. For some references an additional correction is applied (Table 7). The mean error of each individual

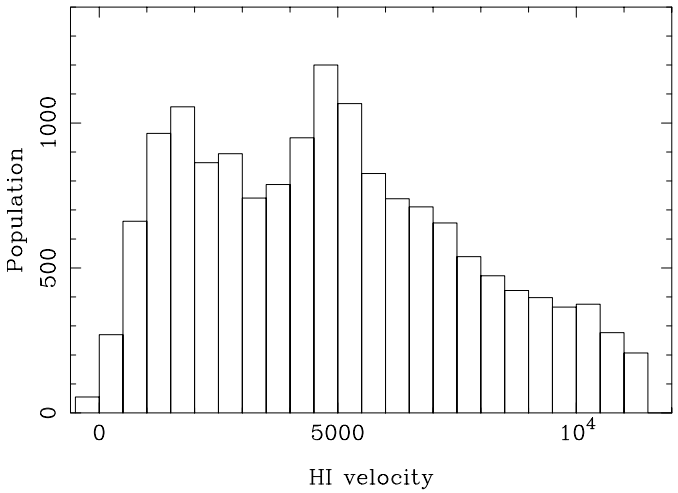

Fig. 4. Distribution of heliocentric radial velocities.

measurement is also calculated as previously stated (Tables 6 or 7). The HI heliocentric radial velocities are not transformed (except one reference that is transformed into the optical definition and one that is corrected for a small scale effect). The mean error of each measurement is calculated as a funtion of the velocity resolution. For unknown velocity resolution we adopted a mean standard deviation of 15 km s^{-1}.

Finaly, for each galaxy the weighted mean and its actual error are calculated. This actual error (Paturel et al. 1997) takes into account the accuracy of each individual source of data and the dispersion of the considered measurements. It gives a realistic description of the uncertainty attached to each mean value. Note that some data receive a flag (:) to show that they may include a discrepant measurement. As far as possible, discordant measurements are rejected (typically when there are several measurements in agreement and one discordant). In order to show the quality of the data the histograms of actual errors on $\log 2V_{\rm M}^{\sin i}$, m_{21} and $v_{\rm HI}$ are given in Fig. 5. The beginning of the final catalog is given in Table 8. This catalog is available in electronic form at the CDS.

Acknowledgements. We thank R. Garnier for helping us in the selection of references and the observers of the Nançay radiotelescope for their contribution to the observations. We thank Dr. J. J. Gallagher III for very useful comments on the manuscript.

Appendix A: New Nançay observations

In this section we present the HI follow-up of a set of galaxies selected in the infrared (IRAS) and near-infrared (DENIS) with the aim of starting to build of a TF catalogue in *BIJHK* bands. This survey is the preliminary step of the present cosmological key-project of the refurbished Nançay radiotelescope, KLUN+, which intends to collect new HI profiles of some 8000 galaxies in the period 2001–2005, on the basis of a DENIS and 2-MASS target selection.

Objects have been selected according to their IRAS flux, $S_{60} > 0.6$ Jy, and/or their I magnitude, $I < 14.5$. Radial velocities where known except for some galaxies at low galactic latitude (211 objects with $|b| < 20°$).

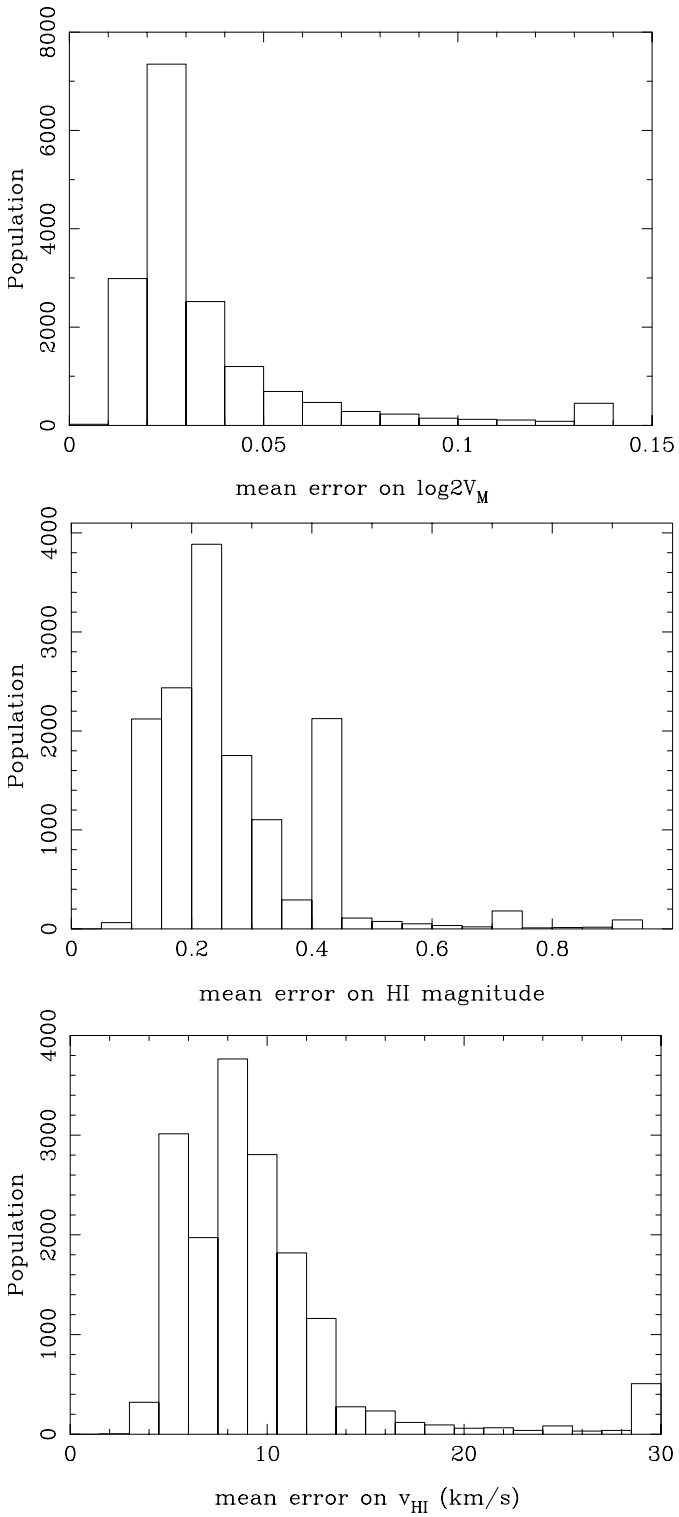

Fig. 5. Distribution of mean errors on $\log 2V_{\rm M}^{\sin i}$, m_{21} and $v_{\rm HI}$.

The present catalogue contains the HI profile and parameters (velocity measurements, 21-cm line widths, HI fluxes, signal to noise ratio, and rms noise) for 817 spiral galaxies.

All these observations have been carried out between 1994 and 1998 with the old system of the meridian-transit Nançay radiotelescope (France). This instrument is a single dish antenna with a collecting area of 6912 m^2 equivalent to that of a

Table 8. The final catalog of homogenized HI data. The catalog gives these data for 16 781 galaxies. The full catalog is available in electronic form at the CDS. **Col. 1:** PGC number from LEDA; **Col. 2:** Alternate name from LEDA; **Col. 3:** Right Ascension and Declination for the equinox 2000, in hours, minutes, seconds and tenths, and degrees, arcminutes and arcseconds; **Col. 4:** Mean homogenized decimal logarithm of twice the maximum rotation velocity uncorrected for inclination ($V_{\rm M}^{\sin i}$ in km s^{-1}); **Col. 5:** Mean homogenized 21-cm magnitude (see Eq. (3)); **Col. 6:** Mean homogenized HI heliocentric radial velocity (in km s^{-1}); Each parameter is given with a flag f telling if it is uncertain ($f = 1$).

PGC	Name	RA(2000)DEC(2000)	log2V_M^sini	f	m21	f	VHI~	f
PGC0000002	UGC12889	J000001.6+471629	2.641+/-0.031	0	15.30+/- 0.39	0	5017.+/- 9.	0
PGC0000006	CGCG456-13	J000002.1+155253	2.312+/-0.024	0	17.73+/- 0.15	0	6001.+/- 10.	0
PGC0000004	KUG2357+228	J000003.4+230516	2.151+/-0.028	0	16.69+/- 0.25	0	4461.+/- 8.	0
PGC0000010	MCG0-01-015	J000007.7-000228	1.825+/-0.048	0	16.55+/- 0.27	0	7099.+/- 9.	0
PGC0000012	MCG-1-01-016	J000008.6-062226	2.560+/-0.027	0	15.97+/- 0.09	0	6547.+/- 8.	0
PGC0000016	MCG-1-01-017	J000011.3-050932	2.424+/-0.032	0	17.09+/- 0.25	0	5669.+/- 8.	0
PGC0000020	MCG0-01-016	J000012.7+010711	2.335+/-0.030	0	16.57+/- 0.32	0	7390.+/- 8.	0
PGC0000029	CGCG517-10	J000022.4+343658	2.101+/-0.057	0	17.47+/- 0.19	0	12702.+/- 10.	0
PGC0000035	UGC12894	J000022.5+392944	1.500+/-0.070	0	15.68+/- 0.13	0	334.+/- 5.	0
...	...	...						
...	...	...						
...	...	...						

Table A.1. New observations. (The full table is available in electronic form at the CDS). **Col. 1:** PGC number from LEDA; **Col. 2:** Alternate name from LEDA; **Col. 3:** Right Ascension and Declination for the equinox 2000, in hours, minutes, seconds and tenths, and degrees, arcminutes and arcseconds; **Col. 4:** 21-cm line width at 20% of the maximum (in km s^{-1}); **Col. 5:** 21-cm line width at 50% of the maximum (in km s^{-1}); **Col. 6:** HI heliocentric radial velocity (in $km.s^{-1}$); **Col. 7:** HI flux (area of the 21-cm line) (in mJy km s^{-1}); **Col. 8:** Signal to Noise ration; **Col. 9:** Quality of the line (see text) and notes (see Table A.3).

PGC name	Name	RA(2000)DEC(2000)	V20 km/s	rms	W20 km/s	rms	W50 km/s	rms	F(HI) mJy.km/s	rms	S/N	Notes	
PGC0000312	8ZW 3	000505.2-07 05 37	3809	4	326	13	306	9	13.64	1.36	10.1	A	*
PGC0166381	IRAS00059+5514	000833.9-55 30 39	5155	4	161	12	148	8	5.80	0.85	9.2	A	
PGC0000789	ESO 349- 38	001112.6-33 34 43	7868	20	589	59	485	39	4.33	0.71	5.2	B	
PGC0000902	MCG -1- 1-52	001334.6-05 05 29	5411	14	345	43	319	29	3.97	0.97	3.6	A	
PGC0001011	NGC 54	001507.7-07 06 25	5337	8	415	25	401	16	3.42	0.59	4.6	A	
PGC0138161	IRAS00156+1658	001817.8-17 14 48	5757	10	429	31	424	20	1.72*	0.67	2.2	C	
PGC0001431	KUG 0019-016	002221.4-01 20 44	4893	3	165	9	71	6	9.04	0.41	34.3	C	C
PGC0001434	UGC 212	002223.1-01 18 12	4868	3	108	10	56	7	6.29	0.58	22.1	C	C
PGC0001534	MCG -1- 2- 9	002428.2-03 51 21	4309	6	279	18	258	12	3.17*	0.46	7.7	B	
...	...	...											
...	...	...											
...	...	...											

94 m-diameter parabolic dish. The half-power beam width at 21-cm is 3.6 arcmin (EW) × 22 arcmin (NS) (at zero declination). Observations where limited to declination $\delta > -38.5°$.

The minimal system temperature at $\delta = 15°$ was about 37 K in both horizontal and vertical polarizations. The spectrometer was a 1024-channel autocorrelator of 6.4 MHz bandwidth. The spacing of the channels corresponds to 2.6 km s^{-1} at 21 cm with a bank of 512 channels in each polarization. After boxcar smoothing the final resolution is typically 10 km s^{-1}. In the velocity-search mode the 1024 channels are split in four banks of 256 channels leading to a range of 4800 km s^{-1} (generally from 400 to 5200 km s^{-1} or from 5200 to 10 000 km s^{-1}). The gain of the antenna has been calibrated according to Fouqué et al. (1990).

Table A.2. Periods of gain stability and correction factors (= $F_0/F_{\rm HI}$).

before June 30th 1991	0.943
Jul. 1991–Oct. 1992	1.000
Nov. 1992–Nov. 1994	1.143
Dec. 1994–Nov. 1995	1.290
Dec. 1995–Nov. 1996	1.449
Dec. 1996–Jun. 1999	1.508

We used the Nançay processing package SIR (Système Interactif de Réduction). The processing chain consist of a selection of good observation cycles (one "observation" is a series of on/off observational sequences), the straightening of the

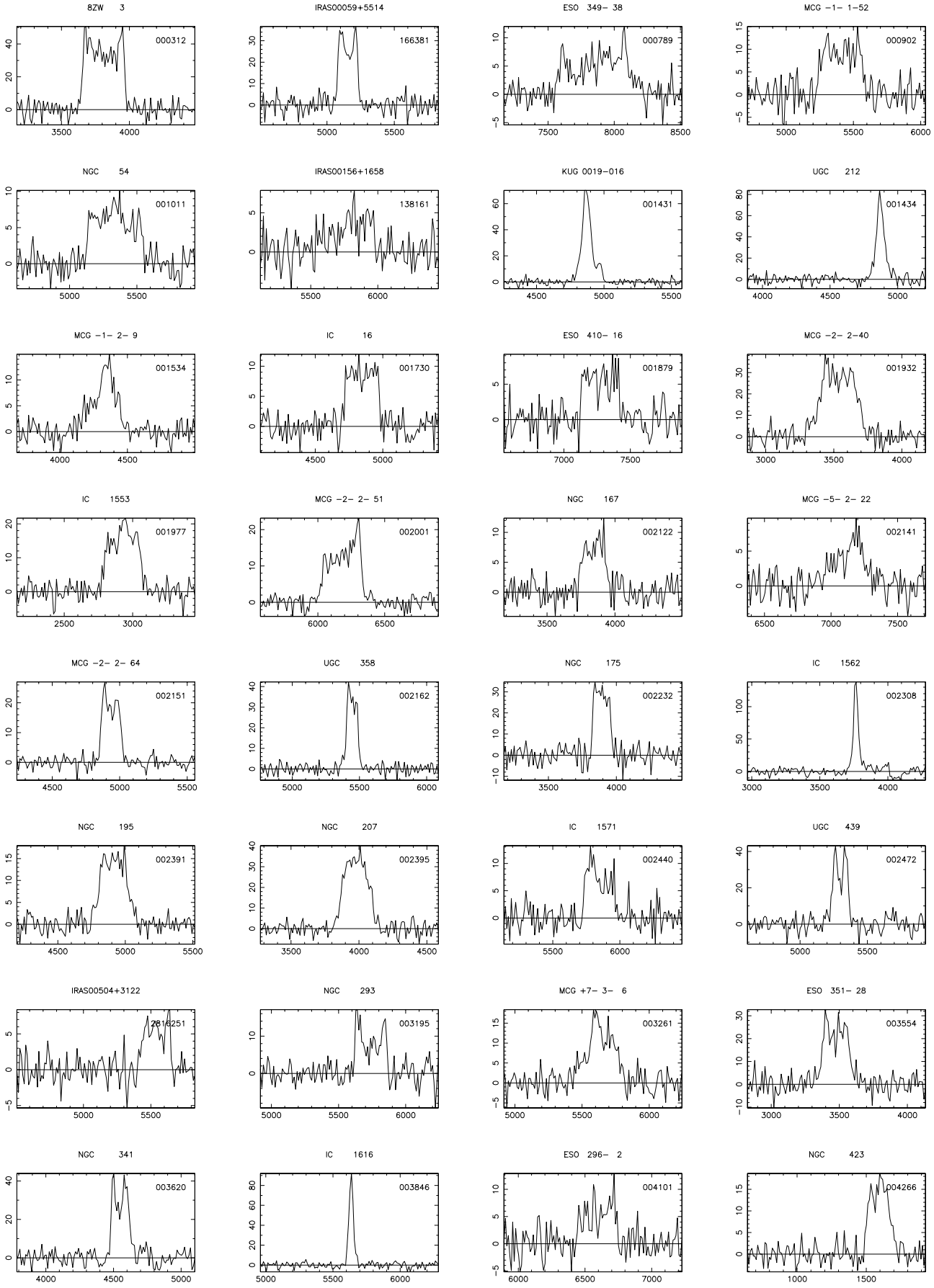

Fig. A.1. Sample of the 21-cm line profiles. The full figure is availaible in the electronic version at `http://www.edpsciences.org`

Table A.3. Comments on some galaxies. The full table is available in electronic form at the CDS. The references concerning these comments are given at the end of the table.

PGC	Name	Comments
PGC0000312	8ZW 3	measured while pointing towards PGC351, 2.5 arcmin northwards
PGC0001431	KUG 0019-016	HI˜confusion with PGC1434
PGC0001434	UGC 212	HI˜confusion with PGC1431
PGC0004878	MCG +7- 3- 29	HI˜confusion with PGC4901 at V=5913 and PGC4915 (Sc RC3) at V=5868
PGC0002308	IC 1562	probably HI˜confusion with PGC2305 (V=3897, barred Sb (DaCosta1998) or Sc (Loveday1996)) in the beam about 4 arcmin south
PGC0005335	CGCG 385-135	HI˜confusion with PGC73964 (Sc Dressler1980) at V=5513 and PGC169815 at V=5586
PGC0005960	ESO 297- 11	HI˜confusion with PGC5959 (SO-a Prugniel1998, Sc Loveday1996) at V=5263
...	...	...
...	...	...
...	...	...

base-line by a polynomial fit, and the application of a boxcar smoothing. The maximum of the line is determined by eye as the mean value of the maxima of each profile's horn after taking into account the medium noise (evaluated in the base-line). The widths, measured at the standard levels 20% and 50% of that maximum, correspond to the "distance" separating the two external points of the profile at these intensity levels.

Together with some other large HI surveys in Nançay, all the data are presented in the on-line Nançay HI extragalactic database (`http://klun.obs-nancay.fr`). The observed radial velocities are listed in Table A.1 (Col. 6) and correspond to the median point of the 21-cm line profile measured at 20% of maximum intensity and translated into the optical velocity scale. The average uncertainty on V_{20} is about 8 km s^{-1} and does not exceed 20 km s^{-1}.

The widths W_{20} and W_{50} are expressed in km s^{-1} (Table A.1, Cols. 4 and 5) and correspond to direct measurements on the 21-cm profiles.

HI-fluxes $F_{\rm HI}$ (Table A.1, Col. 7) are expressed in Jy km s^{-1} and calibrated using as a reference a set of 9 calibrators regularly observed during the survey period (see Theureau et al. 1998). The evolution of the ratio $F_{\rm HI}/F_0$ with time allows us to supervise the Nançay system and to get for each observation the optimal flux measurement. In total, six periods of gain stability have been considered, with corresponding flux correction factors (see Table A.2). From this table and the number of ON/OFF integration cycles observed in each period for a given object, we have been able to correct the flux measurement for each galaxy. Each measurement has been corrected for the Nançay beam effect when position angle, diameter and axis ratio were known (beam-uncorrected flux are flagged with a star).

HI profiles have been classified in four classes according to their quality:

A. high signal to noise, symmetrical, double horn profile, best data for TF application;
B. robust HI parameters for TF application, more noisy than "A" galaxies;
C. well detected but noisy profile, generally HI confused, but OK for radial velocity measurement;
D. marginally detected, not useful.

General notes, mainly concerning possible or confirmed HI-confusion with some identified companion, are given in Table A.1.

References

Bicay, M. D., & Giovanelli, R. 1986, AJ, 91, 705
Bothun, G. D., Aaronson, M., Schommer, R. A., et al. 1985, ApJS, 57, 423
Bottinelli, L., Gouguenheim, L., Fouqué, P., & Paturel, G. 1990, A&AS, 82, 391
Bottinelli, L., Gouguenheim, L., & Paturel, G. 1982, A&A, 113, 61
Dickel, J. R., & Rood, H. J. 1978, ApJ, 223, 391
Fisher, J. R., & Tully, R. B. 1981, ApJS, 47, 139
Fouque, P., & Bottinelli, L., & Durand, N., et al. 1990, A&AS, 86, 473
Giovanelli, R., Avera, E., & Karachentsev, I. D. 1997, AJ, 114(1), 122
Giovanelli, R., Haynes, M. P., Myers, S. T., & Roth, J. 1986, AJ, 92, 250
Giovanelli, R., & Haynes, M. P. 1985, AJ, 90, 2445
Giovanelli, R., & Haynes, M. P. 1989, AJ, 97, 633
Giovanelli, R., & Haynes, M. P. 1993, AJ, 105(4), 1271
Haynes, M. P., Giovanelli, R., Chamaraux, P., Da Costa, L. N., et al. 1999, AJ, 117, 2039
Haynes, M. P., Giovanelli, R., Herter, T., et al. 1997, AJ, 113(4), 1197
Haynes, M. P., Giovanelli, R., Starosta, B. M., et al. 1988, AJ, 95, 607
Haynes, M. P., & Giovanelli, R. 1991, ApJS, 77, 331
Hoffman, G. L., Helou, G., Salpeter, E. E., et al. 1987, ApJS, 63, 247
Huchtmeier, W. K., Karachentsev, I. D., Karachentseva, V. E., et al. 2000, AAS, 141, 469
Impey, C. D., Burkholder, V., & Sprayberry, D. 2001, AJ, 122, 2341
Lewis, B. M., Helou, G., & Salpeter, E. E. 1985, ApJS, 59, 161
Lewis, B. M. 1987, ApJS, 63, 515
Lu, N. Y., & Freudling, W. 1995, ApJ, 449, 527
Lu, N. Y., Hoffman, G. L., Groff, T., et al. 1993, ApJS, 88, 383

Mathewson, D. S., & Ford, V. L. 1996, ApJS, 107, 97
Matthews, L. D., & van Driel, W. 2000, A&AS, 143, 421
Paturel, G., Andernach, H., Bottinelli, L., et al. 1997, A&AS, 124, 109
Paturel, G., Fouqué, P., Buta, R., & Garcia, A. M. 1991, A&A, 243, 319
Paturel, G., Petit, C., Prugniel, Ph., et al. 2003, A&A, 412, 45 (Paper I)
Peterson, S. D. 1979, ApJS, 40, 527
Richter, O. G., & Huchtmeier, W. K. 1991, A&AS, 87, 425
Rosenberg, J. L., & Schneider, S. E. 2000, ApJS, 130, 177
Rubin, V. C., Ford Jr., W. K., Thonnard, N., et al. 1976, AJ, 81, 687
Schneider, S. E., Thuan, T. X., Mangum, J. G., et al. 1992, ApJS, 81, 5
Shostak, G. S. 1978, AA, 68, 321
Staveley-Smith, L., & Davies, R. D. 1988, MN, 231, 833
Theureau, G., Bottinelli, L., Coudreau-Durand, N., et al. 1998, A&AS, 130, 333
Thuan, T. X., & Seitzer, P. O. 1979, ApJ, 231, 327
Tifft, W. G., & Cocke, W. J. 1988, ApJS, 67, 1-75
Tully, R. B., & Fisher, J. R. 1977, A&A, 54, 661
Vaucouleurs, G. de, Vaucouleurs, A. de, Corwin, H. G., et al. 1991, RC3 (Springer-Verlag)
Wegner, G., Haynes, M. P., & Giovanelli, R. 1993, AJ, 105, 1251

Online Material

Table 4. Correction of $\log W(r,l)$ to $\log 2V_M^{\sin i}$. This table gives the conversion coefficients and the mean error for the 26 subsamples (level and resolution). l is the level code (see Table 2). r is the mean velocity resolution in km s^{-1}.

l	r	$a \pm \sigma_a$	$b \pm \sigma_b$	σ	n	N_s
5	8	1.071 ± 0.009	−0.210 ± 0.023	0.044	928	2933
1	8	1.187 ± 0.002	−0.543 ± 0.005	0.036	5309	8952
1	21	1.193 ± 0.005	−0.563 ± 0.012	0.043	1438	9371
5	21	1.049 ± 0.002	−0.158 ± 0.005	0.033	3003	11 381
5	16	1.048 ± 0.003	−0.156 ± 0.006	0.025	1591	11 952
5	41	1.052 ± 0.009	−0.176 ± 0.021	0.051	751	14 687
1	16	1.179 ± 0.003	−0.529 ± 0.008	0.038	2065	15 028
1	41	1.156 ± 0.010	−0.521 ± 0.025	0.068	1047	15 785
8	16	1.124 ± 0.003	−0.376 ± 0.007	0.028	2412	15 815
6	8	1.146 ± 0.005	−0.450 ± 0.010	0.028	477	16 212
4	41	1.120 ± 0.011	−0.384 ± 0.027	0.043	447	16 408
2	8	1.145 ± 0.003	−0.430 ± 0.007	0.024	720	16 408
4	21	1.093 ± 0.005	−0.280 ± 0.012	0.019	251	16 412
4	8	1.088 ± 0.006	−0.266 ± 0.014	0.015	143	16 412
8	8	1.084 ± 0.006	−0.266 ± 0.015	0.037	538	16 412
7	21	1.278 ± 0.020	−0.827 ± 0.051	0.029	99	16 443
2	21	1.279 ± 0.059	−0.786 ± 0.149	0.057	40	16 447
4	16	1.087 ± 0.006	−0.260 ± 0.013	0.015	121	16 447
7	16	1.226 ± 0.016	−0.677 ± 0.041	0.027	112	16 447
8	21	1.126 ± 0.007	−0.390 ± 0.017	0.028	465	16 457
9	8	1.107 ± 0.012	−0.339 ± 0.031	0.027	155	16 467
9	16	1.148 ± 0.011	−0.431 ± 0.027	0.024	141	16 554
6	16	1.149 ± 0.016	−0.466 ± 0.041	0.029	126	16 621
9	21	1.181 ± 0.015	−0.524 ± 0.038	0.030	83	16 643
2	41	1.043 ± 0.027	−0.205 ± 0.066	0.038	76	16 686
7	8	1.082 ± 0.039	−0.302 ± 0.098	0.037	27	16 721

Table 5. Correction of $\log 2V_M^{\sin i}$ to the adopted standard (ref. 23286). This table gives the conversion coefficients and the mean error for the 65 references requiring an additional correction.

Ref.	$a \pm \sigma_a$	$b \pm \sigma_b$	σ	n	N_s
23289	1.000 ± 0.000	−0.007 ± 0.002	0.036	390	2439
18000	1.054 ± 0.010	−0.132 ± 0.024	0.024	158	4084
23121	1.026 ± 0.010	−0.058 ± 0.024	0.021	95	5064
23152	1.000 ± 0.000	−0.011 ± 0.004	0.030	51	5121
24372	1.021 ± 0.008	−0.062 ± 0.019	0.028	523	5384
12320	0.958 ± 0.018	0.087 ± 0.043	0.047	119	6019
23171	1.000 ± 0.000	0.020 ± 0.004	0.023	28	6074
27036	1.000 ± 0.000	−0.010 ± 0.004	0.029	54	6081
16120	1.066 ± 0.016	−0.177 ± 0.038	0.048	257	6129
23195	1.000 ± 0.000	−0.016 ± 0.003	0.026	84	6277
23366	1.082 ± 0.024	−0.194 ± 0.053	0.041	57	6424
16121	0.902 ± 0.016	0.250 ± 0.038	0.030	76	7094
12310	1.000 ± 0.000	−0.026 ± 0.008	0.054	45	7268
23302	1.087 ± 0.018	−0.216 ± 0.041	0.030	56	7316
123303	1.000 ± 0.000	−0.029 ± 0.005	0.055	140	7337
12379	1.000 ± 0.000	−0.020 ± 0.009	0.055	36	7391
23296	0.968 ± 0.011	0.063 ± 0.026	0.017	68	7422
23284	1.031 ± 0.011	−0.089 ± 0.026	0.014	80	7931
23087	0.957 ± 0.009	0.097 ± 0.022	0.025	102	8666
23123	1.048 ± 0.005	−0.115 ± 0.010	0.033	467	8791
23092	1.022 ± 0.009	−0.056 ± 0.022	0.019	59	8877
23091	1.032 ± 0.012	−0.083 ± 0.030	0.016	63	9067
23444	0.954 ± 0.022	0.102 ± 0.051	0.063	100	9250
23067	1.000 ± 0.000	−0.024 ± 0.003	0.037	149	9713
16057	1.000 ± 0.000	0.015 ± 0.006	0.053	72	9961
16081	1.071 ± 0.018	−0.193 ± 0.042	0.044	96	10 008
12158	1.053 ± 0.018	−0.126 ± 0.044	0.040	85	10 013
23212	1.029 ± 0.014	−0.086 ± 0.033	0.022	85	10 063
23324	1.000 ± 0.000	−0.013 ± 0.004	0.029	65	10 329
23095	0.922 ± 0.026	0.177 ± 0.062	0.046	58	10 776
23009	1.076 ± 0.018	−0.189 ± 0.042	0.044	136	11 104
23251	1.075 ± 0.011	−0.190 ± 0.026	0.022	133	11 132
23048	1.000 ± 0.000	−0.011 ± 0.002	0.023	99	11 193
12327	0.805 ± 0.053	0.482 ± 0.124	0.058	35	11 395
23232	1.000 ± 0.000	−0.027 ± 0.003	0.026	57	11 454
23321	0.955 ± 0.017	0.105 ± 0.040	0.026	52	11 506
23252	0.843 ± 0.044	0.378 ± 0.108	0.052	28	11 549
16049	1.045 ± 0.017	−0.114 ± 0.038	0.021	41	11 609
23000	1.084 ± 0.014	−0.208 ± 0.033	0.030	68	11 672
23319	0.930 ± 0.034	0.156 ± 0.080	0.042	21	11 725
23231	0.975 ± 0.012	0.055 ± 0.031	0.013	37	11 782
23271	1.000 ± 0.000	−0.019 ± 0.007	0.036	25	11 816
23234	1.000 ± 0.000	0.016 ± 0.005	0.036	49	11 867
12346	0.867 ± 0.035	0.328 ± 0.084	0.061	50	11 876
12393	1.000 ± 0.000	−0.009 ± 0.003	0.029	79	11 921
16100	1.000 ± 0.000	0.029 ± 0.013	0.050	17	11 988
23220	1.000 ± 0.000	−0.031 ± 0.015	0.050	11	12 015
23295	1.000 ± 0.000	−0.041 ± 0.009	0.031	11	12 081
23194	1.000 ± 0.000	−0.017 ± 0.007	0.039	29	12 182
23043	1.000 ± 0.000	0.034 ± 0.005	0.026	32	12 253
23147	0.895 ± 0.031	0.236 ± 0.078	0.031	43	12 257
23360	1.302 ± 0.062	−0.639 ± 0.118	0.068	35	12 287
23352	0.290 ± 0.265	1.738 ± 0.674	0.145	12	12 311
23307	1.258 ± 0.042	−0.715 ± 0.104	0.061	56	12 355
23101	0.917 ± 0.029	0.201 ± 0.065	0.049	36	12 355
23316	0.895 ± 0.052	0.210 ± 0.105	0.043	22	12 373
23332	1.000 ± 0.000	−0.078 ± 0.027	0.104	16	12 397
23120	0.894 ± 0.044	0.262 ± 0.098	0.040	26	12 405
23075	0.951 ± 0.018	0.119 ± 0.048	0.012	14	12 426
23084	0.843 ± 0.036	0.385 ± 0.089	0.028	26	12 434
23198	1.000 ± 0.000	−0.027 ± 0.011	0.042	15	12 441
23237	1.067 ± 0.030	−0.138 ± 0.066	0.021	14	12 478
12234	1.000 ± 0.000	−0.044 ± 0.018	0.071	15	12 490
12275	1.000 ± 0.000	−0.112 ± 0.021	0.074	15	12 490
23081	1.000 ± 0.000	−0.111 ± 0.020	0.079	18	12 492

Table 6. Correction of m_{21} to the scale of Nançay. This table gives the the zero-point shift and the mean error for the different radiotelescope (Col. 1). By its adoption as a standard, the Nançay radiotelescope (t = 1) has $b = 0$ and its standard deviation is $\sigma = 0.24$.

t	$b \pm \sigma_b$	σ	n	N_s
7	0.052 ± 0.016	0.393	647	4182
9	−0.086 ± 0.013	0.415	1043	6413
3	0.051 ± 0.012	0.260	467	12 813
10	0.076 ± 0.015	0.324	448	13 115
5	0.045 ± 0.013	0.261	443	13 947
8	0.073 ± 0.013	0.317	594	13 989
2	−0.026 ± 0.016	0.272	322	14 417
14	−0.036 ± 0.037	0.305	68	14 426
15	0.095 ± 0.036	0.405	136	14 443
11	0.038 ± 0.112	0.515	23	14 497
13	0.088 ± 0.083	0.371	32	14 498
12	−0.036 ± 0.075	0.285	22	14 499
4	−0.069 ± 0.088	0.403	20	14 500
6	0.287 ± 0.174	0.655	13	14 500

Table 7. Correction of m_{21} to the standard (ref. 23289). This table gives the zero-point shift and its mean error for the 46 references requiring an additional correction.

Ref.	$b_r \pm \sigma_{b_r}$	σ	n	N_s
23195	−0.177 ± 0.019	0.147	61	2997
23321	−0.134 ± 0.031	0.183	41	3625
23359	−0.095 ± 0.036	0.266	56	3866
23224	−0.060 ± 0.027	0.200	57	4505
23296	0.082 ± 0.036	0.247	47	4710
23226	0.060 ± 0.025	0.171	55	5770
23239	−0.252 ± 0.041	0.268	42	5960
23200	0.051 ± 0.020	0.263	181	6864
23271	−0.298 ± 0.052	0.206	17	7414
23238	−0.289 ± 0.029	0.267	81	7479
18000	0.039 ± 0.007	0.189	669	7525
23251	−0.065 ± 0.015	0.151	100	7972
27036	−0.098 ± 0.047	0.309	54	8097
16120	0.104 ± 0.020	0.306	305	9378
23444	−0.344 ± 0.049	0.472	94	9495
23097	−0.086 ± 0.027	0.303	123	9654
23009	−0.099 ± 0.021	0.255	150	9795
23337	−0.224 ± 0.096	0.468	24	9836
23067	−0.172 ± 0.018	0.217	144	10 059
23048	0.272 ± 0.031	0.322	111	10 147
23117	−0.090 ± 0.037	0.370	102	10 268
12320	−0.083 ± 0.024	0.277	129	10 543
23213	−0.236 ± 0.081	0.449	32	10 610
12393	0.314 ± 0.059	0.276	86	10 929
23318	0.075 ± 0.037	0.240	48	10 933
23290	0.038 ± 0.011	0.109	95	11 056
23338	−0.204 ± 0.060	0.248	20	11 069
12310	0.286 ± 0.042	0.266	41	11 145
16121	−0.134 ± 0.027	0.250	87	11 196
23302	−0.248 ± 0.044	0.342	63	11 361
23268	0.169 ± 0.067	0.266	32	11 458
23231	0.078 ± 0.035	0.223	46	11 506
23342	−0.095 ± 0.029	0.183	39	11 630
23147	−0.385 ± 0.061	0.322	48	11 664
23329	0.187 ± 0.051	0.315	40	11 684
23279	0.129 ± 0.055	0.309	32	11 714
23187	−0.094 ± 0.041	0.179	18	11 840
23264	0.201 ± 0.057	0.250	18	11 920
23265	−0.156 ± 0.052	0.272	30	11 955
23234	−0.175 ± 0.062	0.368	35	12 069
12232	0.274 ± 0.081	0.416	32	12 131
23363	−0.219 ± 0.050	0.225	22	12 173
16119	0.187 ± 0.075	0.372	27	12 184
23365	−0.240 ± 0.106	0.511	23	12 218
23316	−0.091 ± 0.038	0.182	26	12 224
12157	0.197 ± 0.063	0.303	25	12 277

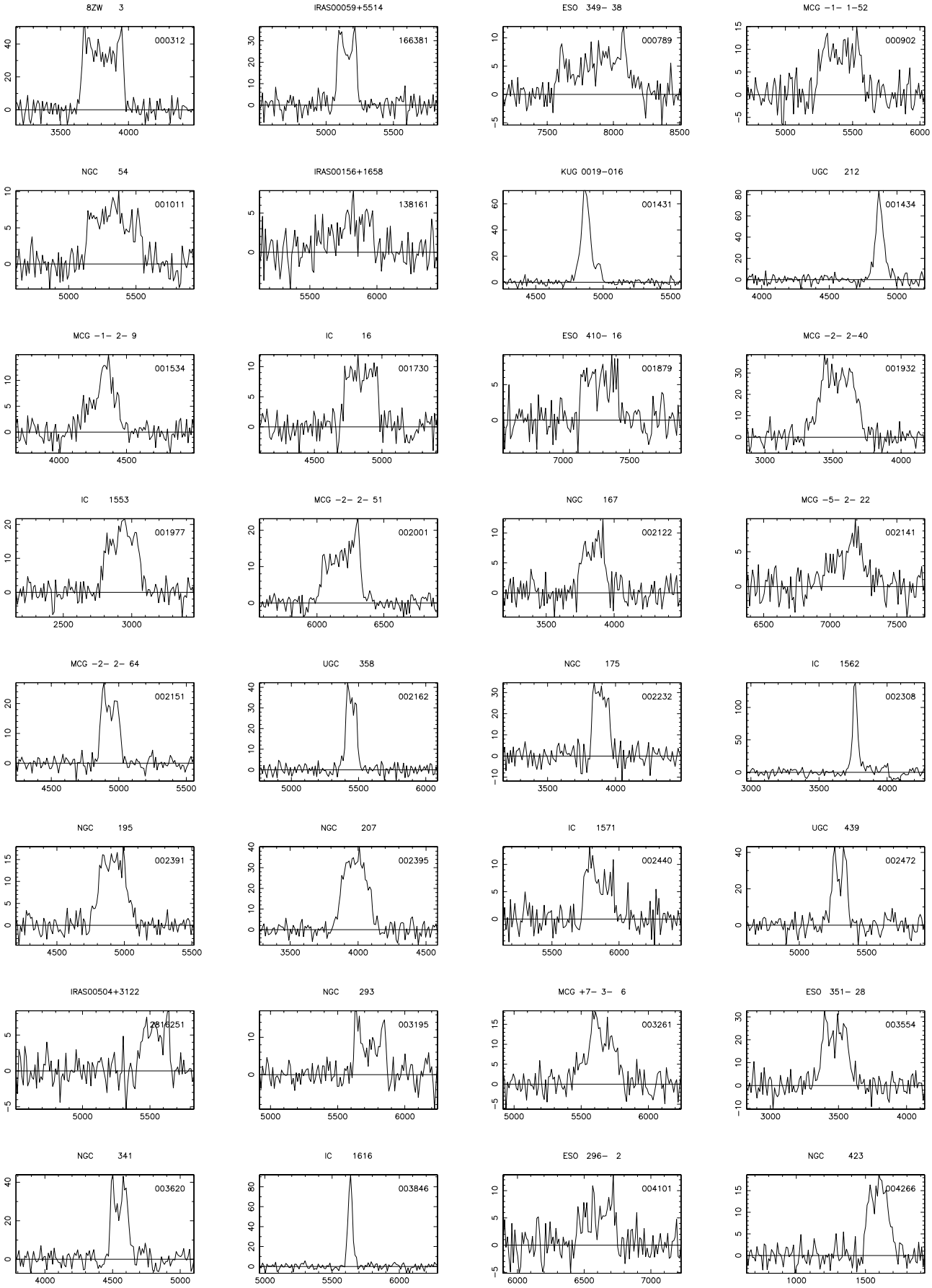

Fig. A.1. Sample of the 21-cm line profiles.

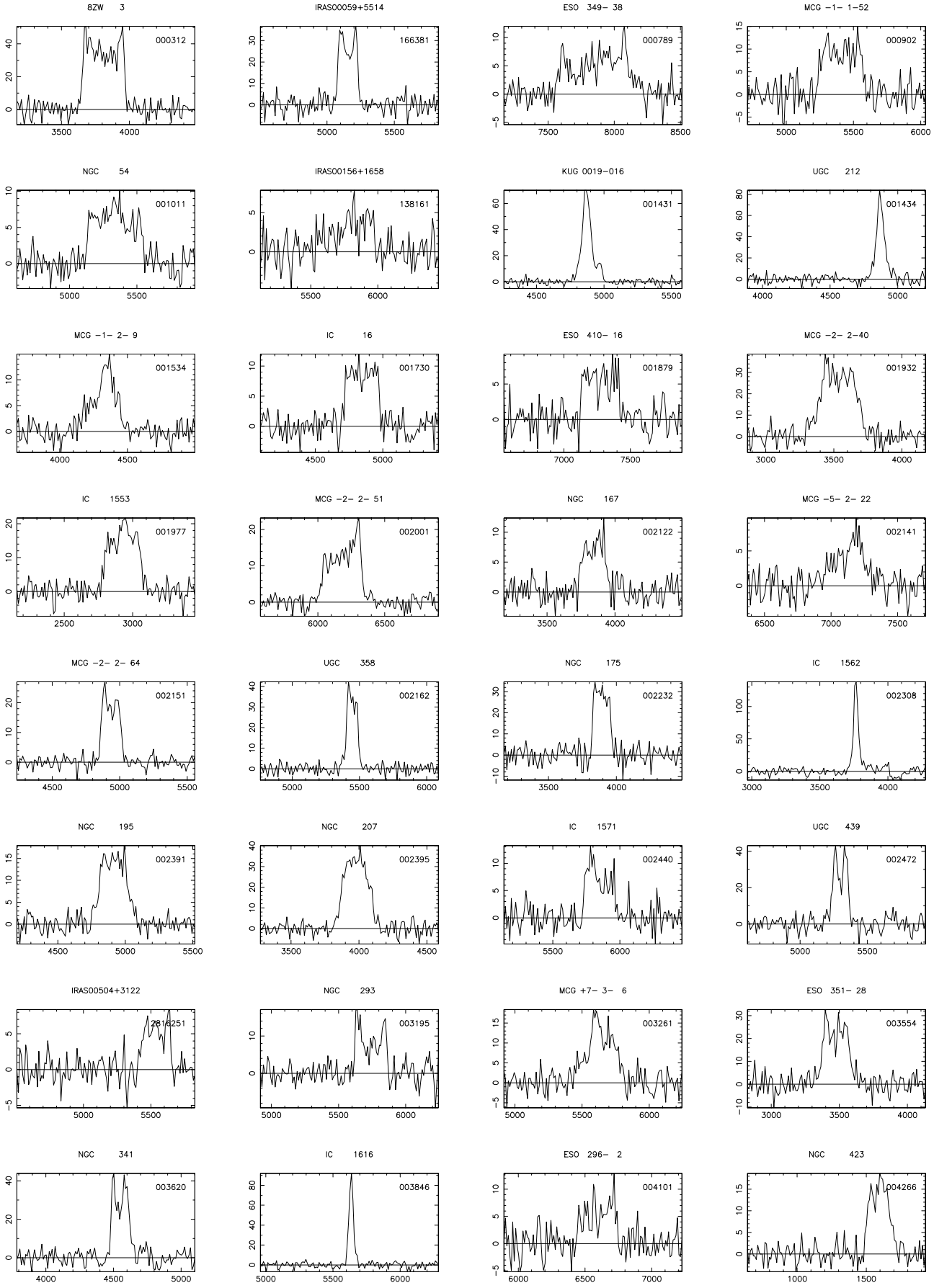

Fig. A.1. continued.

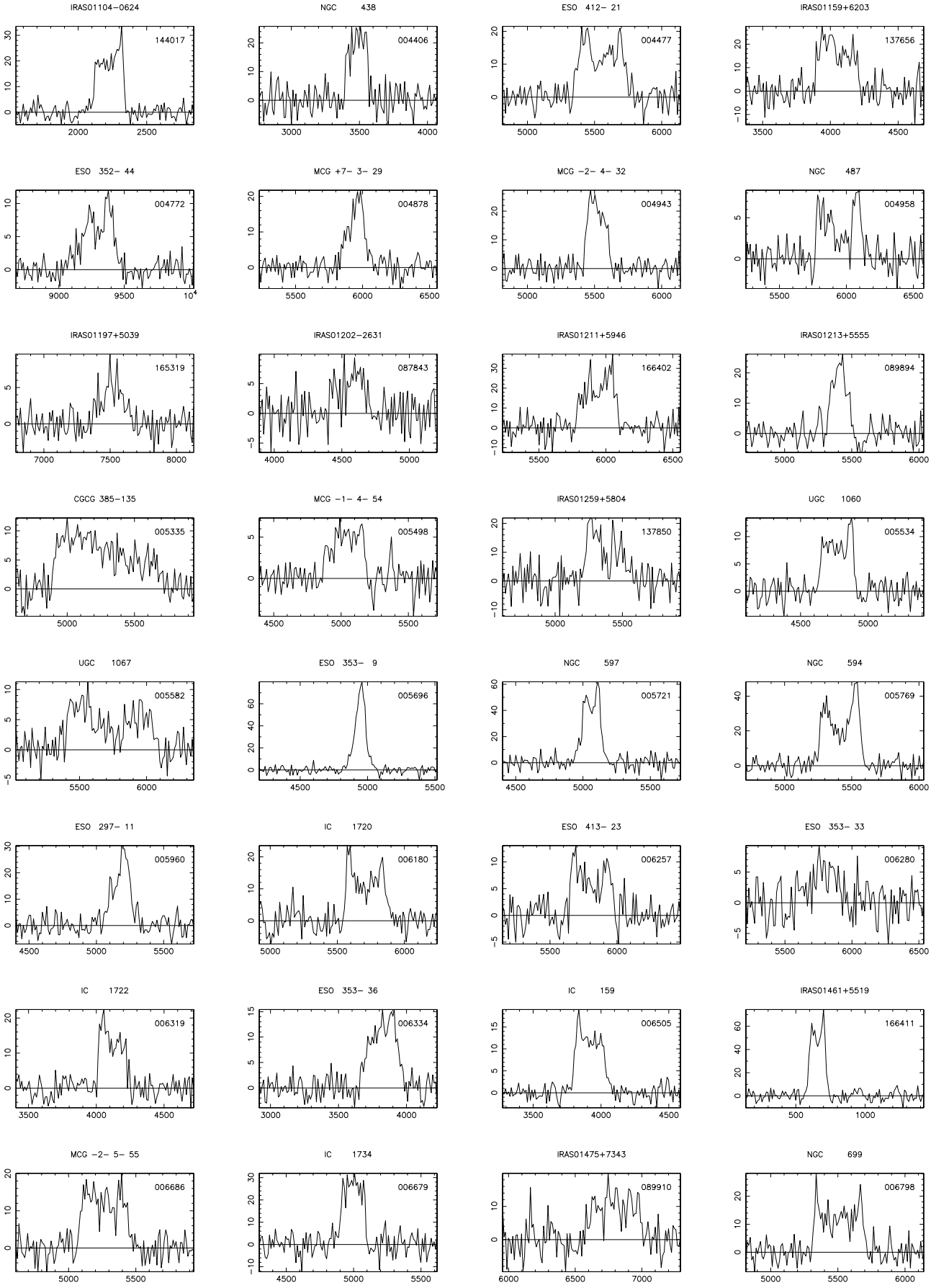

Fig. A.1. continued.

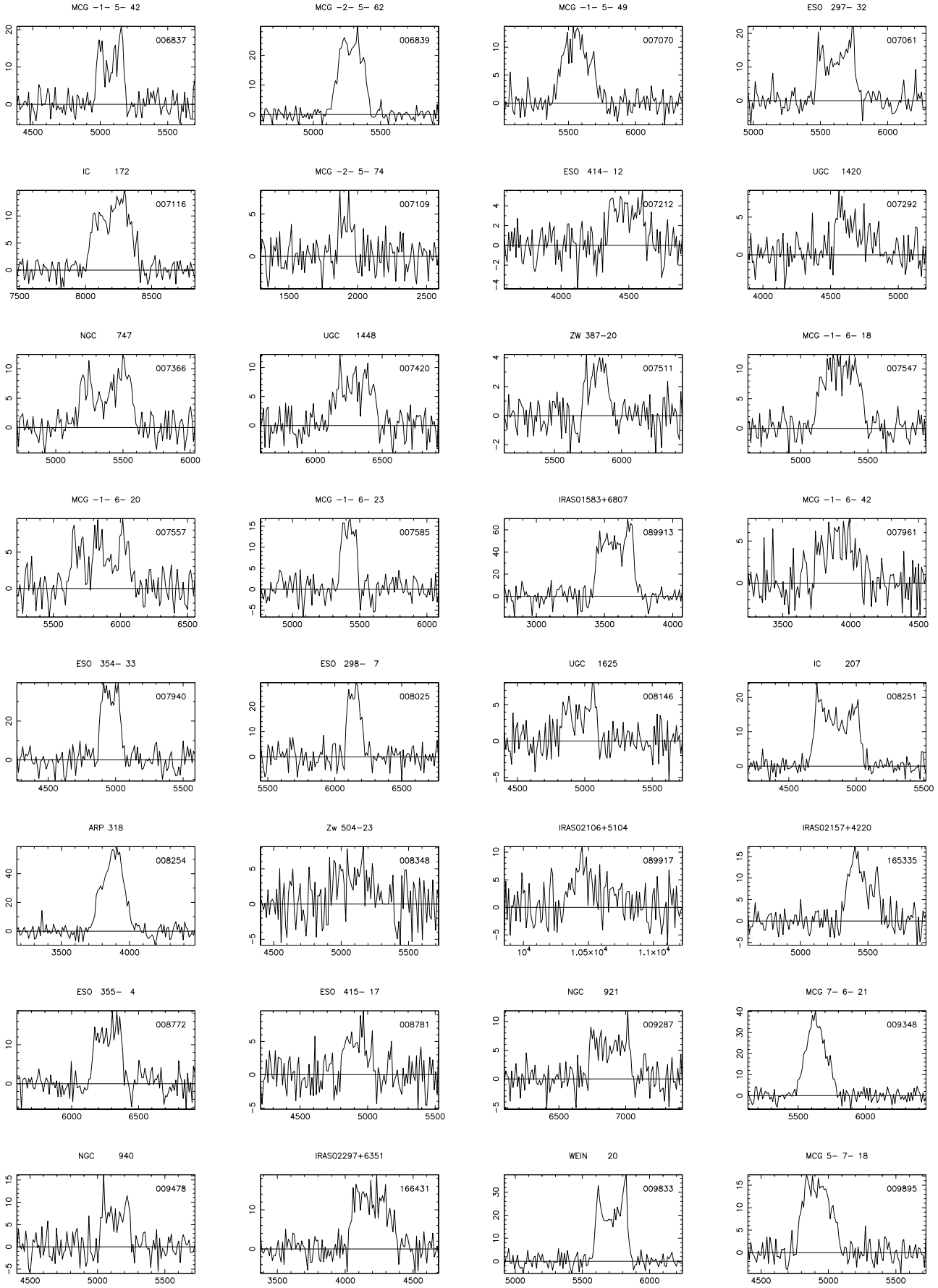

Fig. A.1. continued.

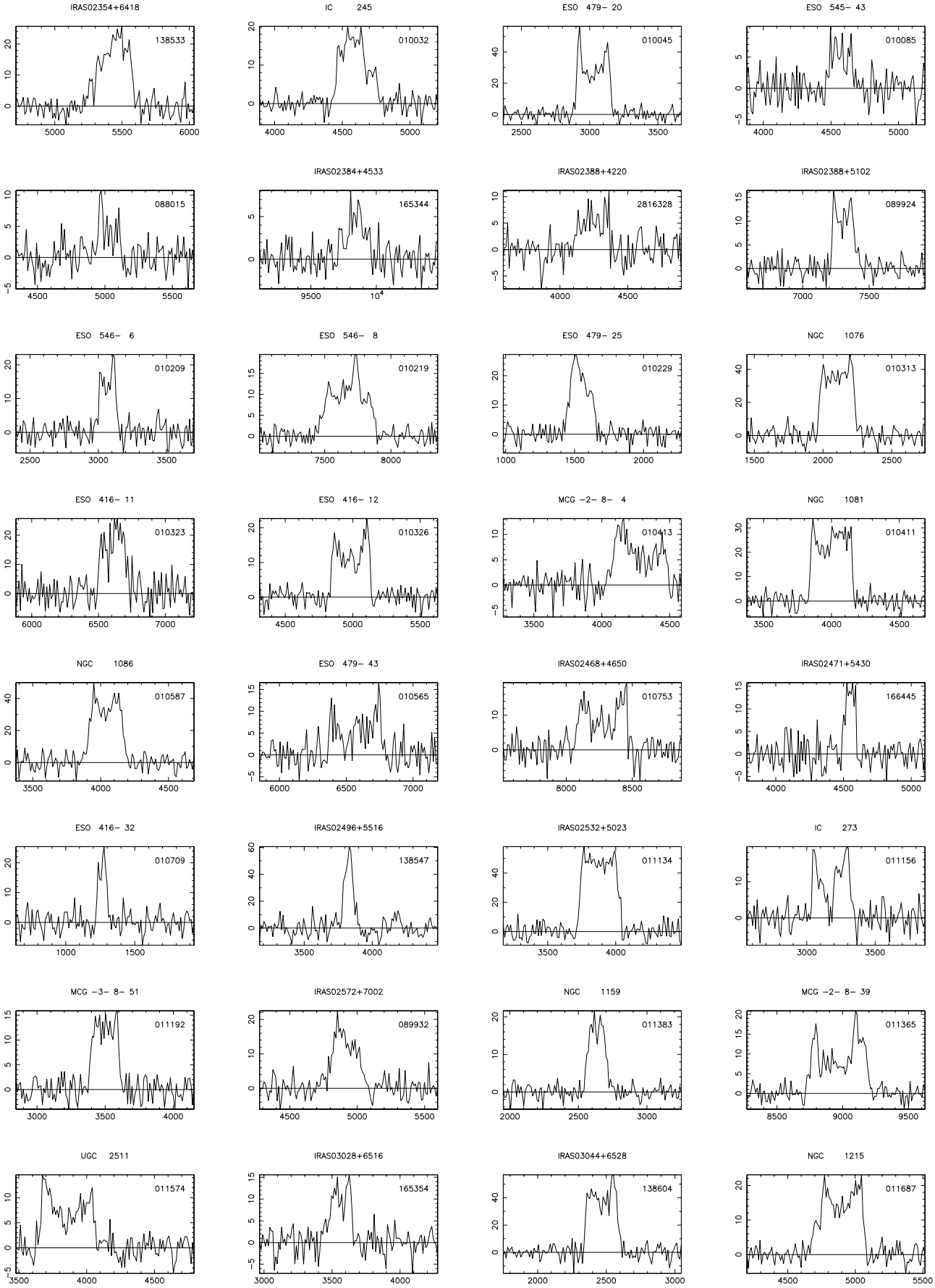

Fig. A.1. continued.

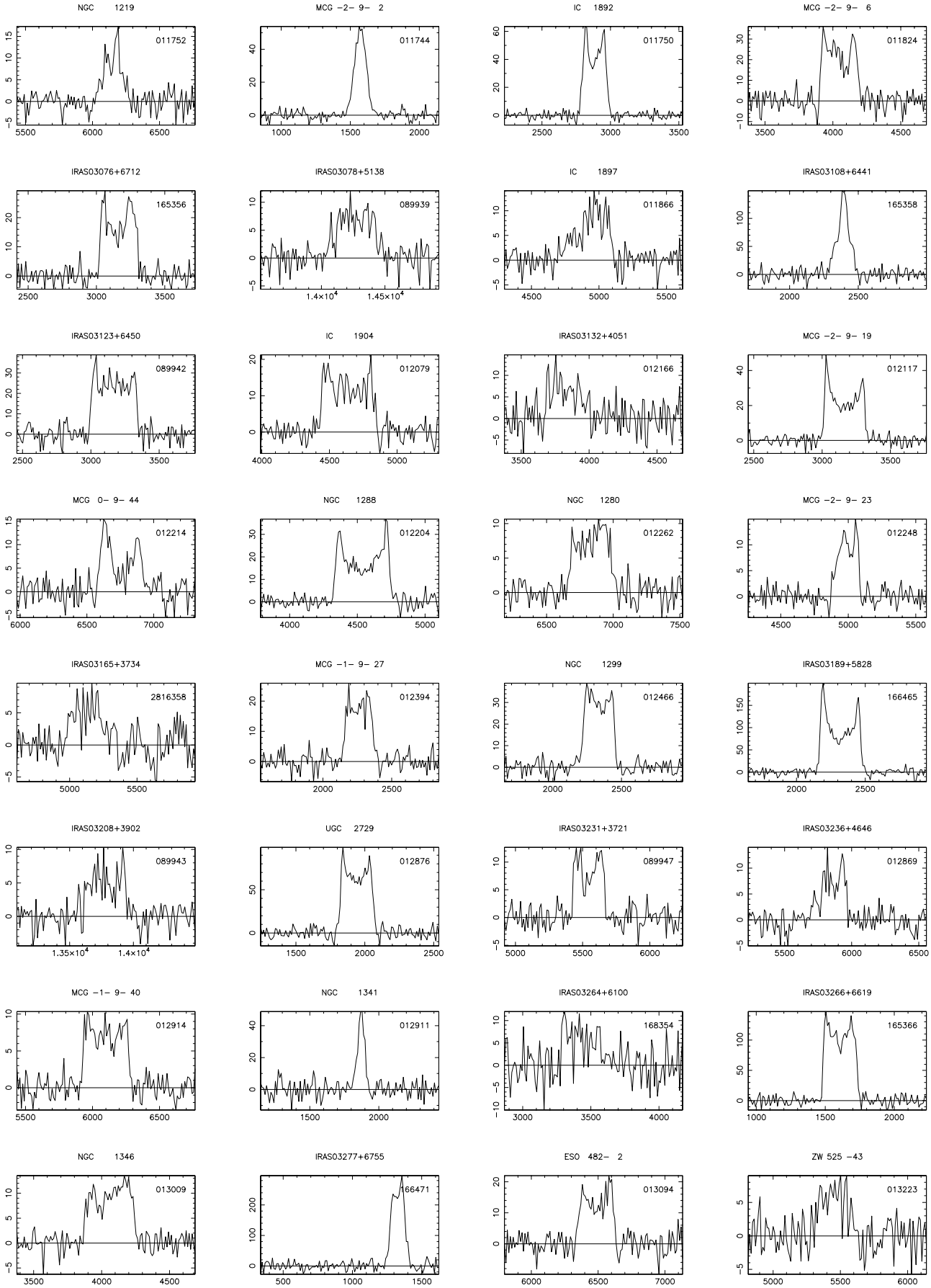

Fig. A.1. continued.

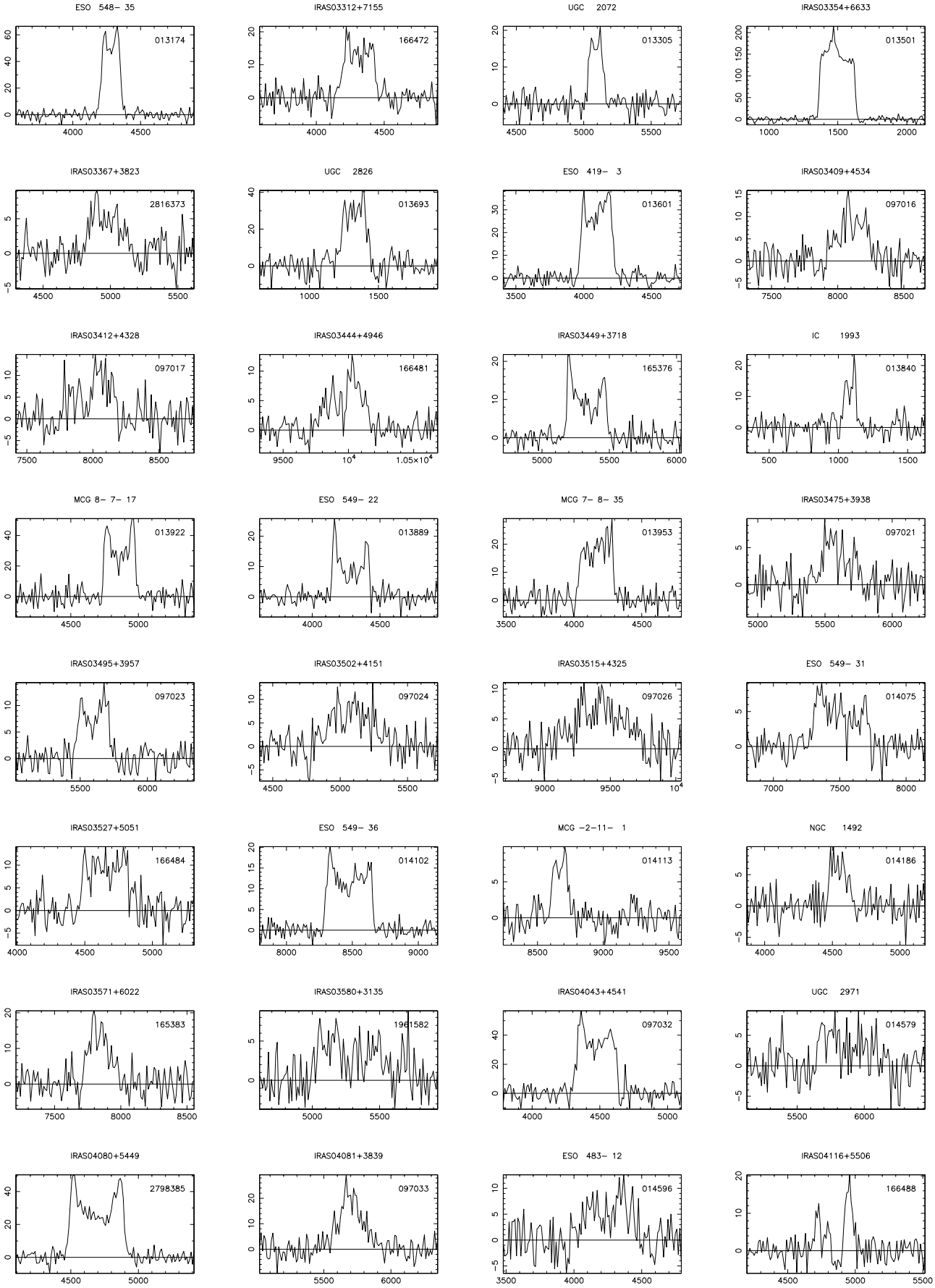

Fig. A.1. continued.

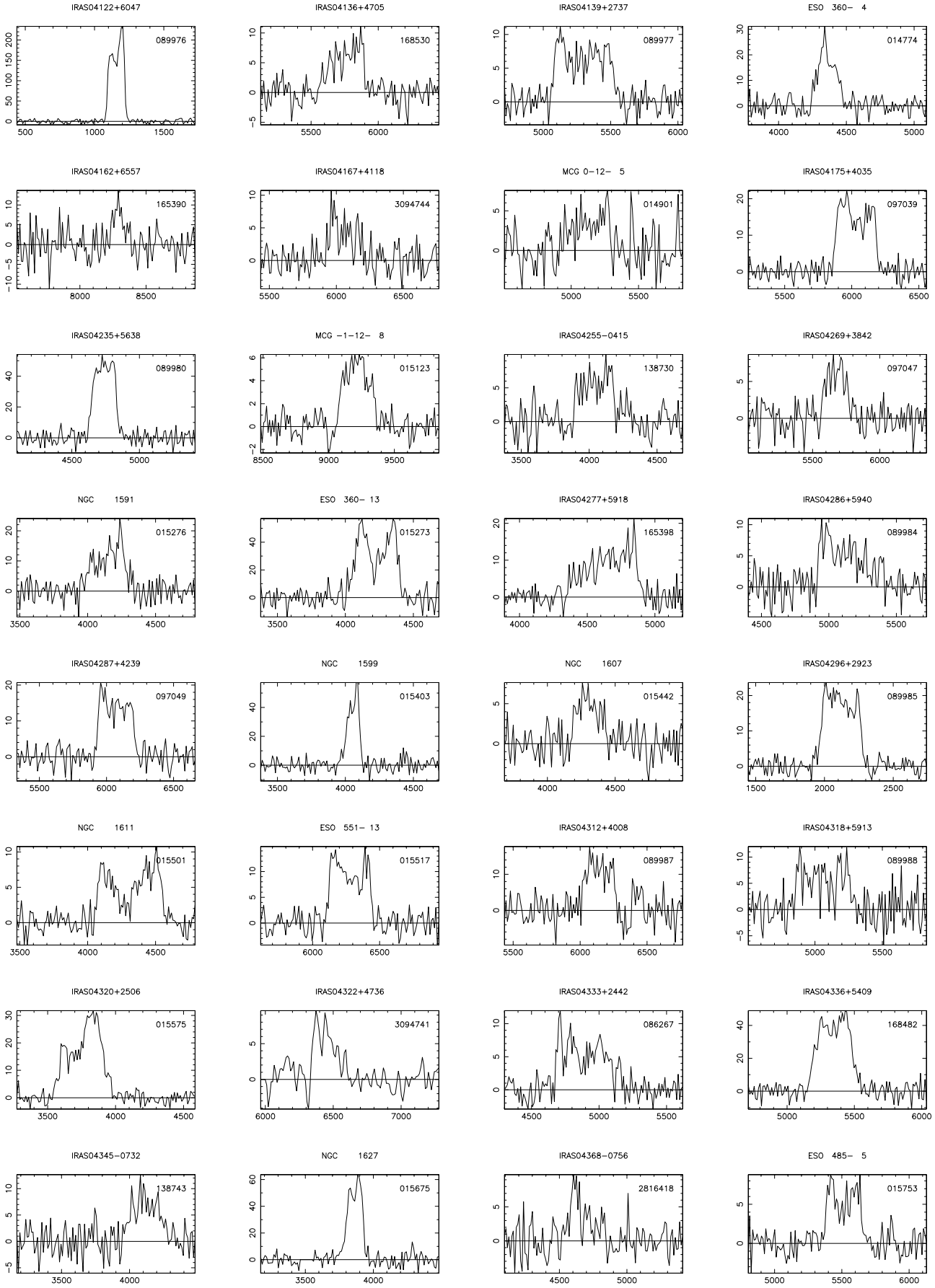

Fig. A.1. continued.

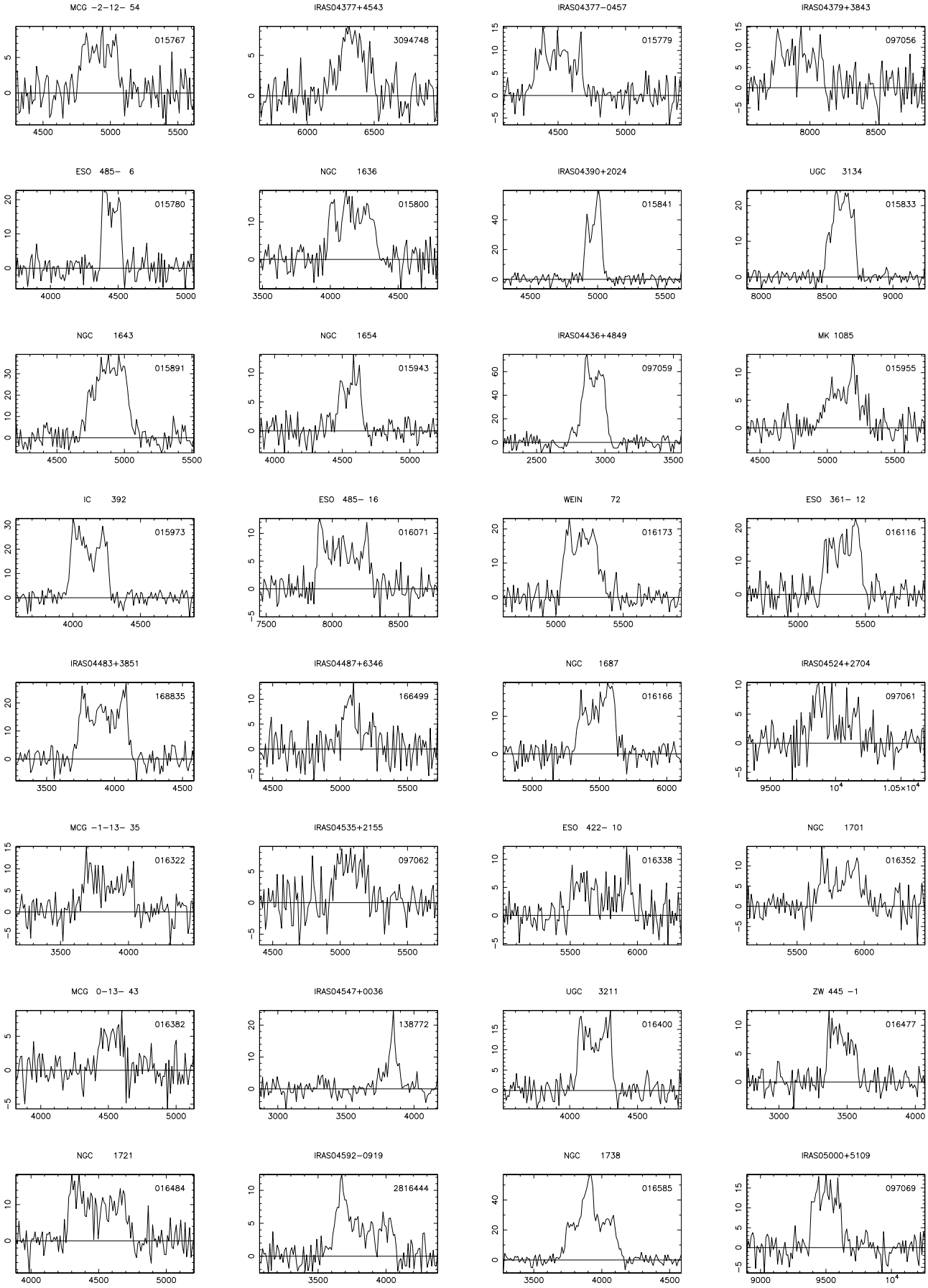

Fig. A.1. continued.

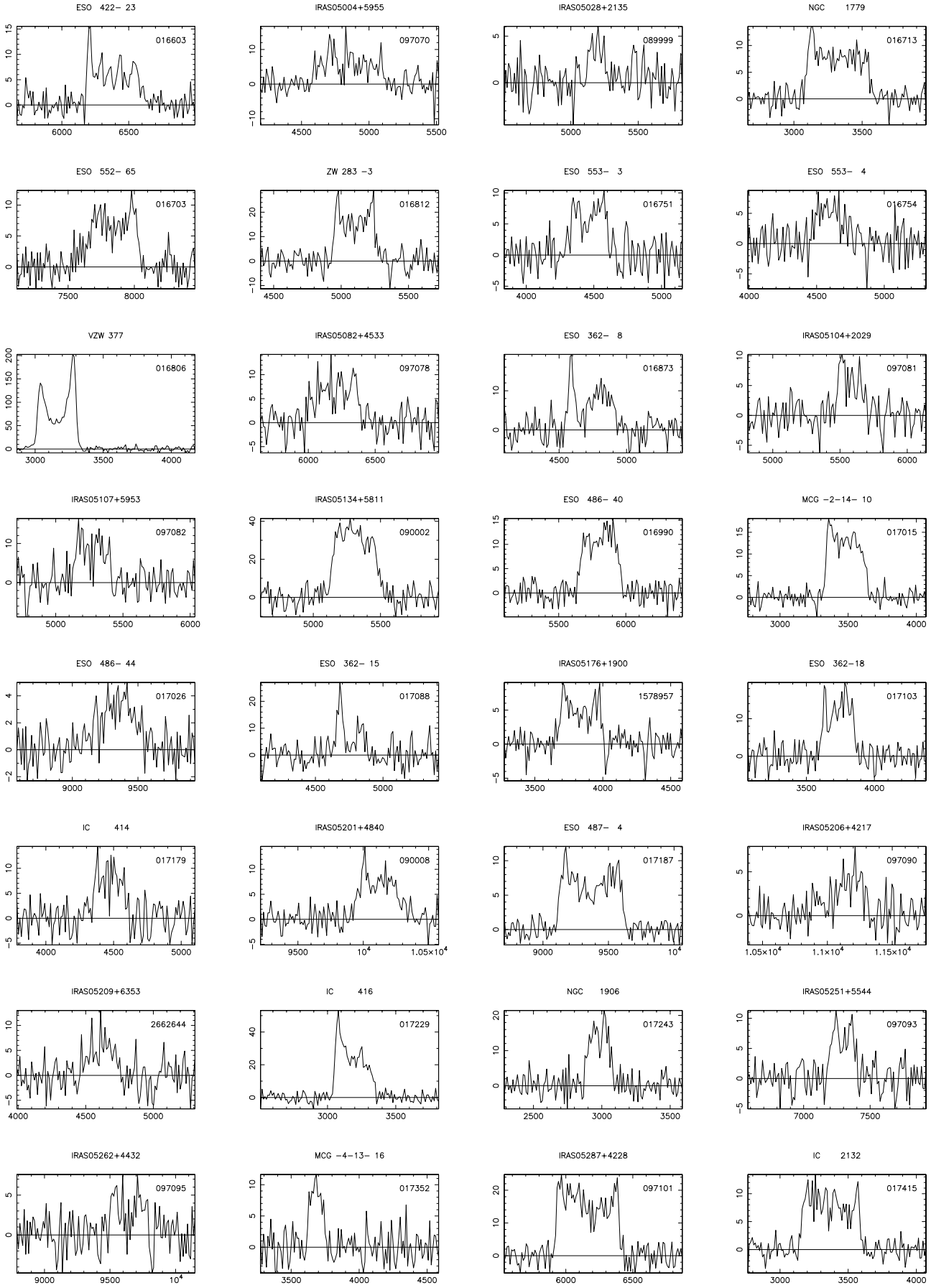

Fig. A.1. continued.

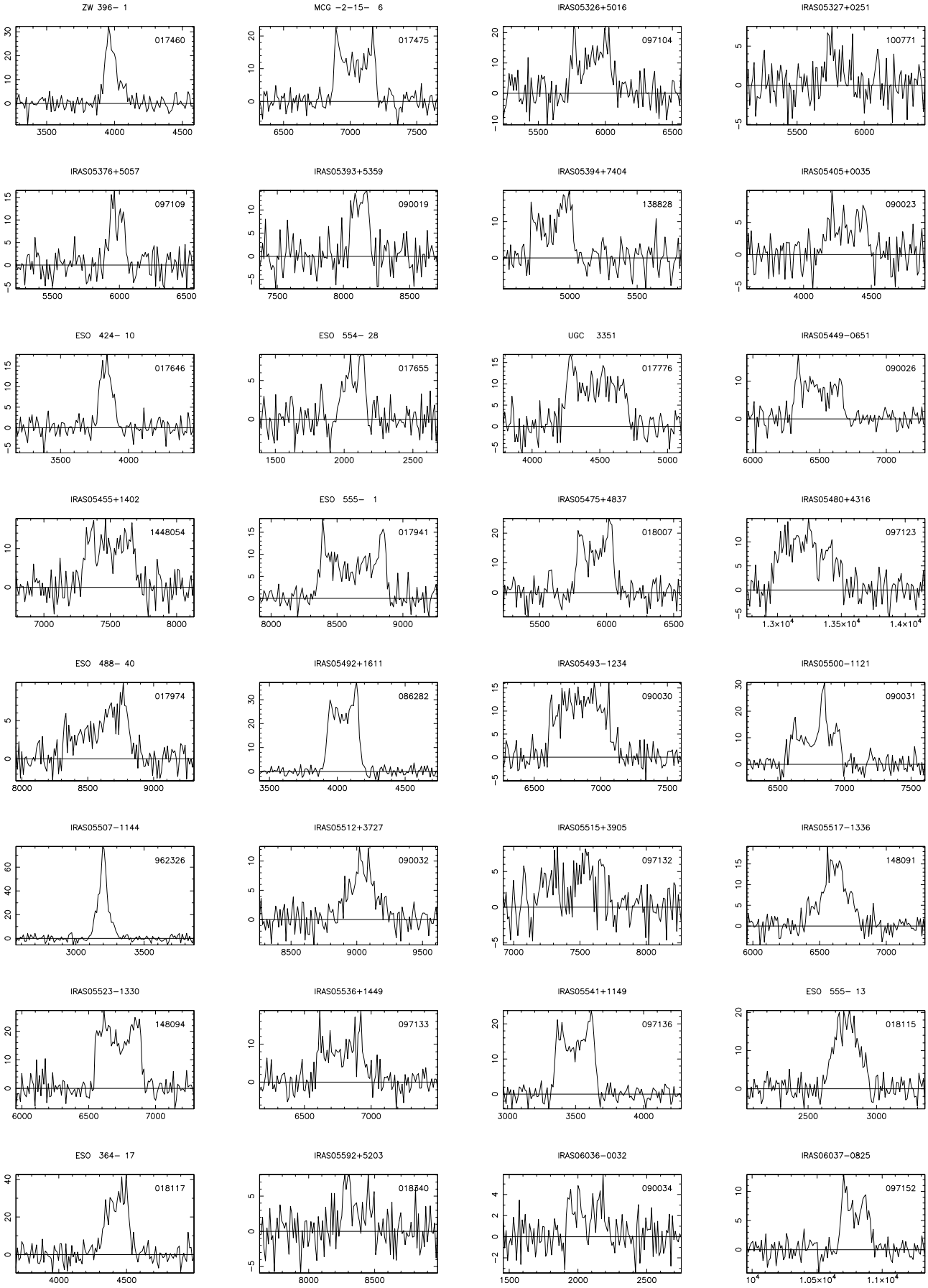

Fig. A.1. continued.

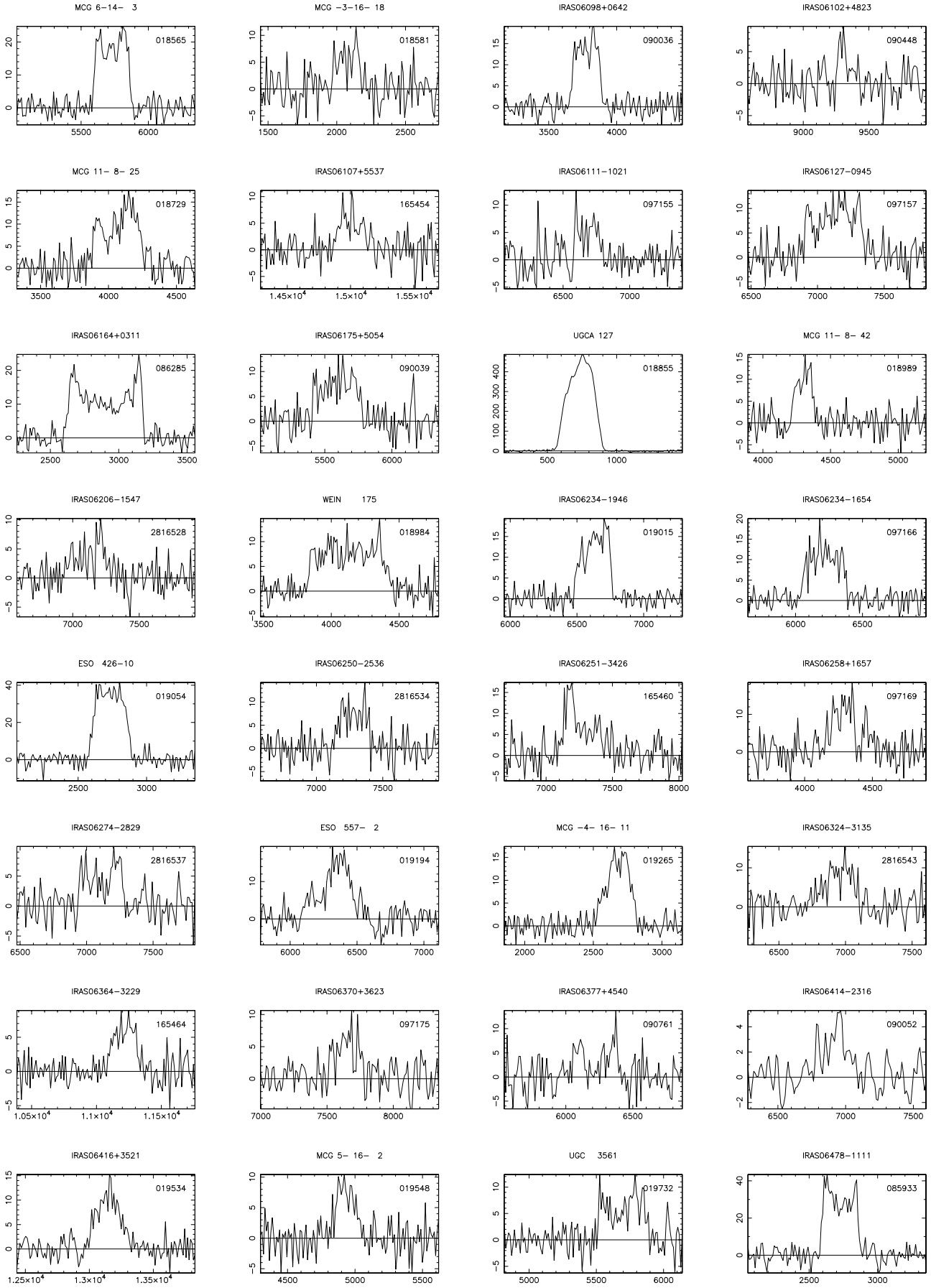

Fig. A.1. continued.

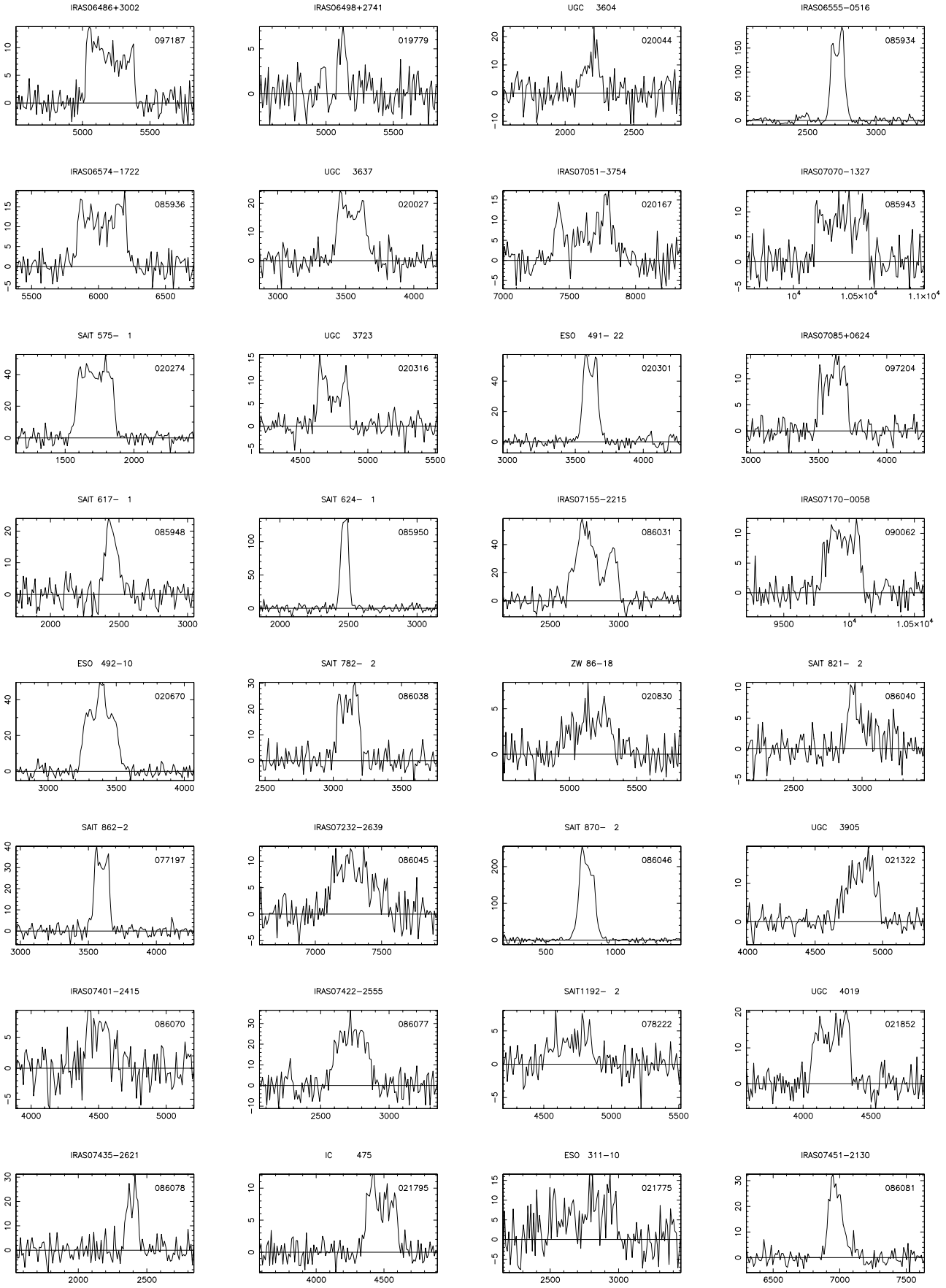

Fig. A.1. continued.

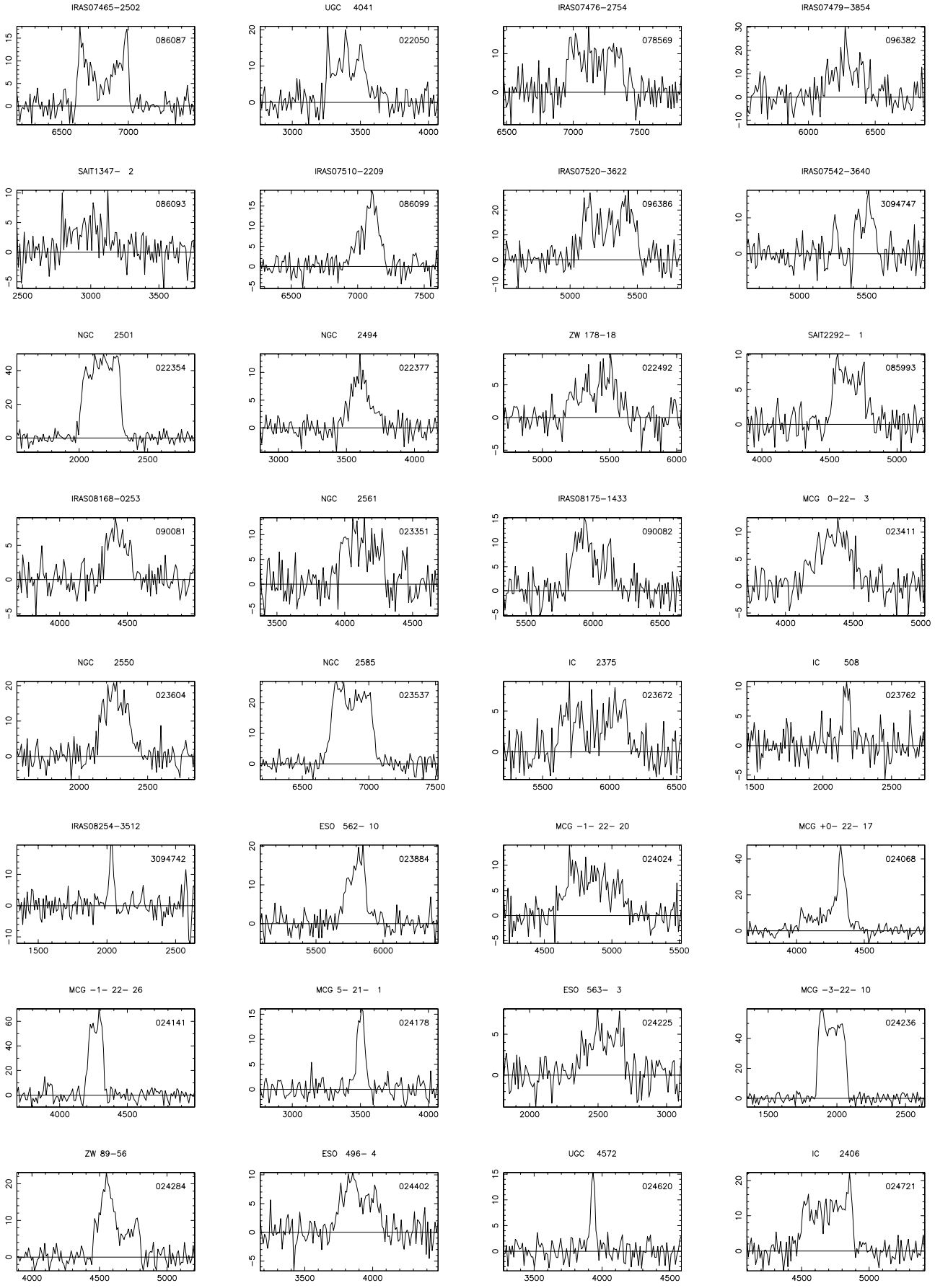

Fig. A.1. continued.

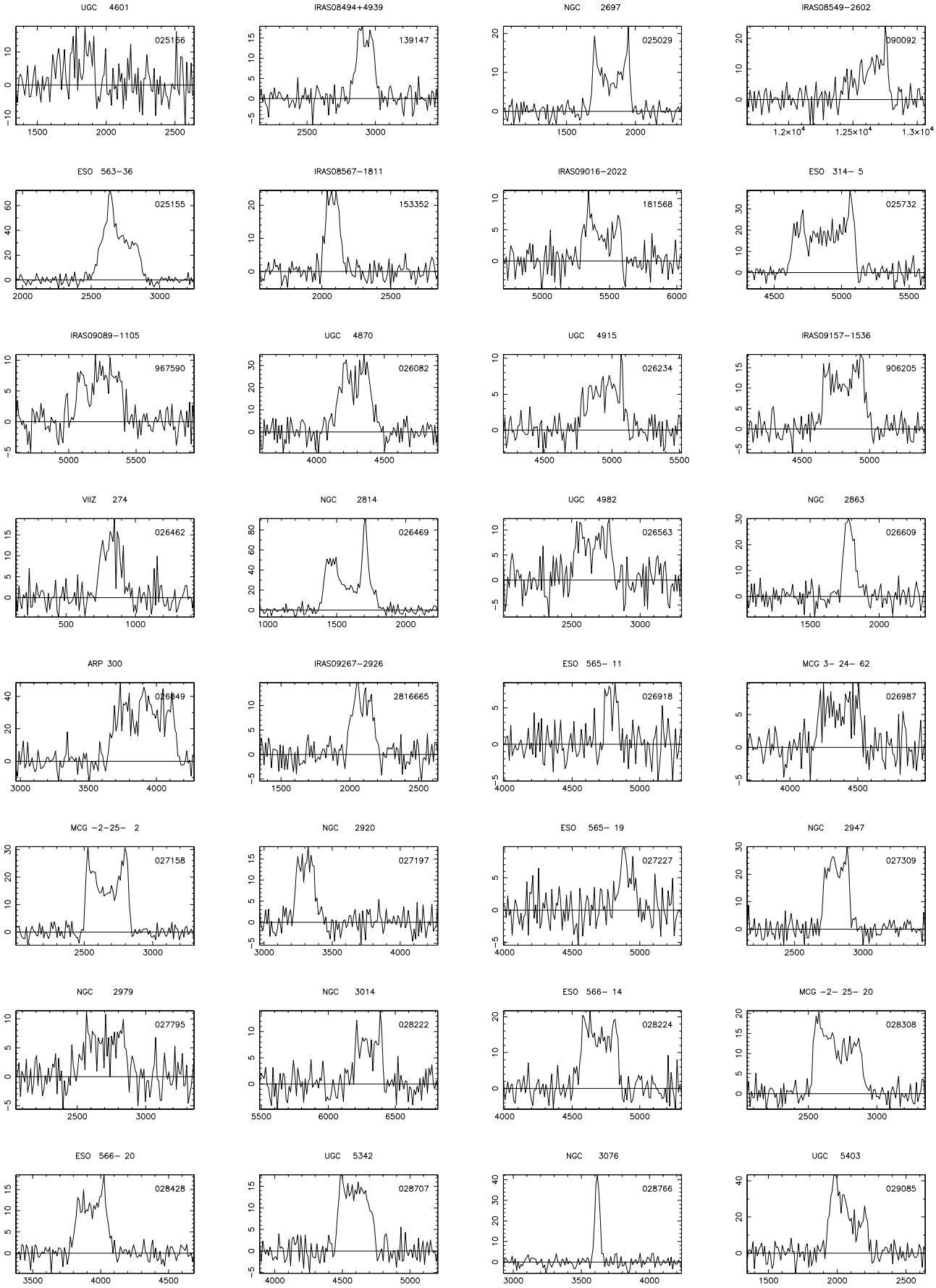

Fig. A.1. continued.

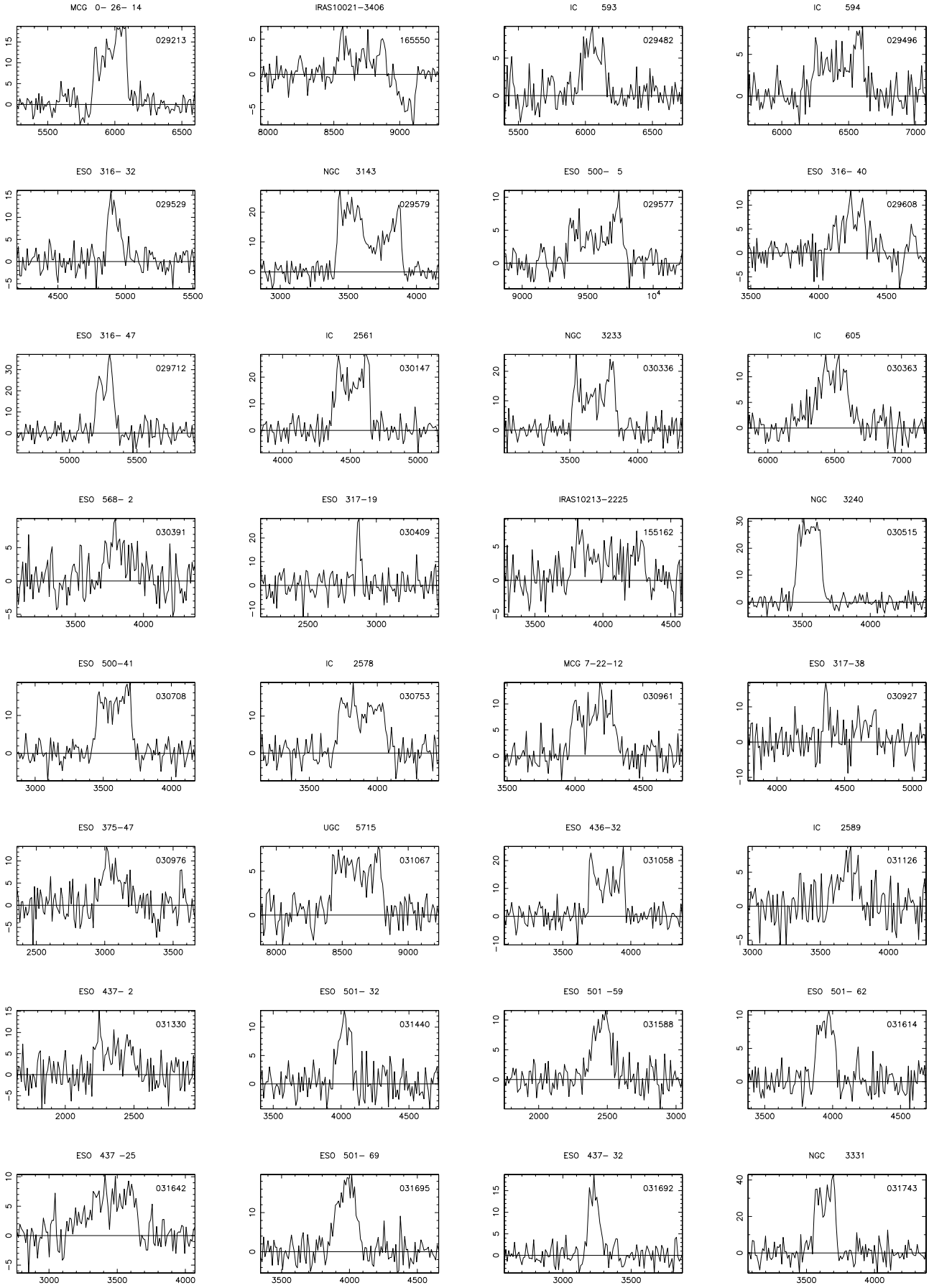

Fig. A.1. continued.

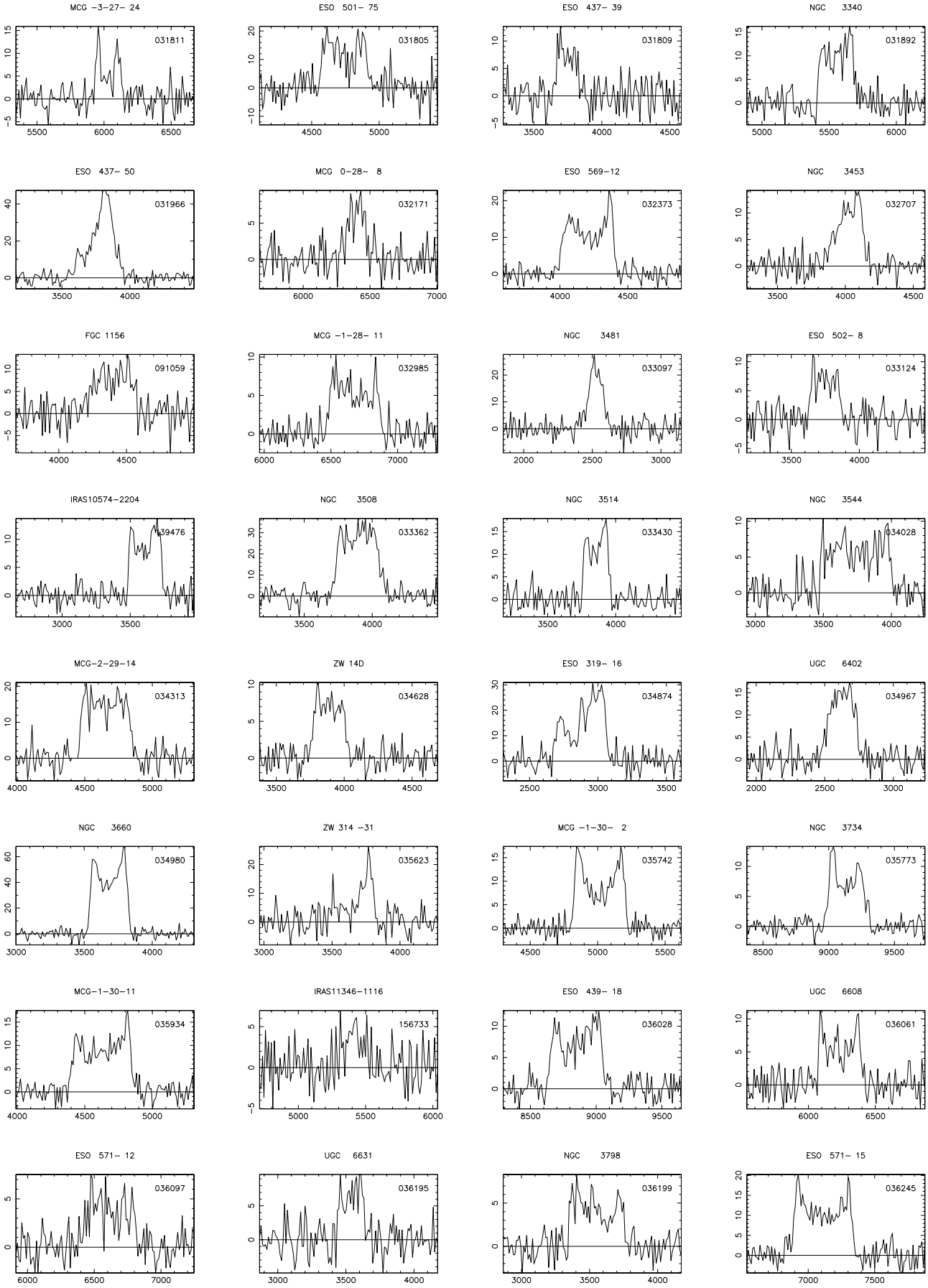

Fig. A.1. continued.

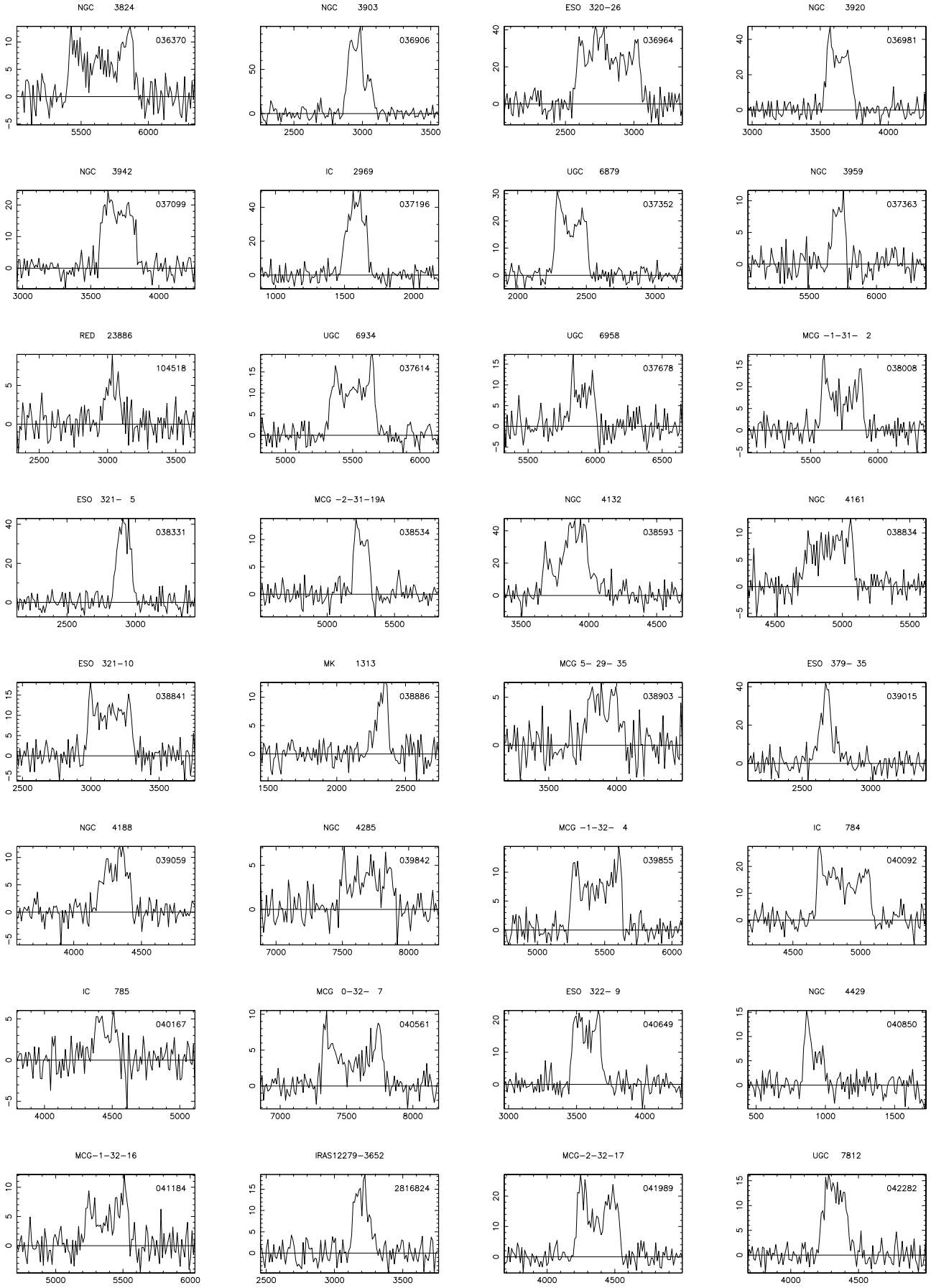

Fig. A.1. continued.

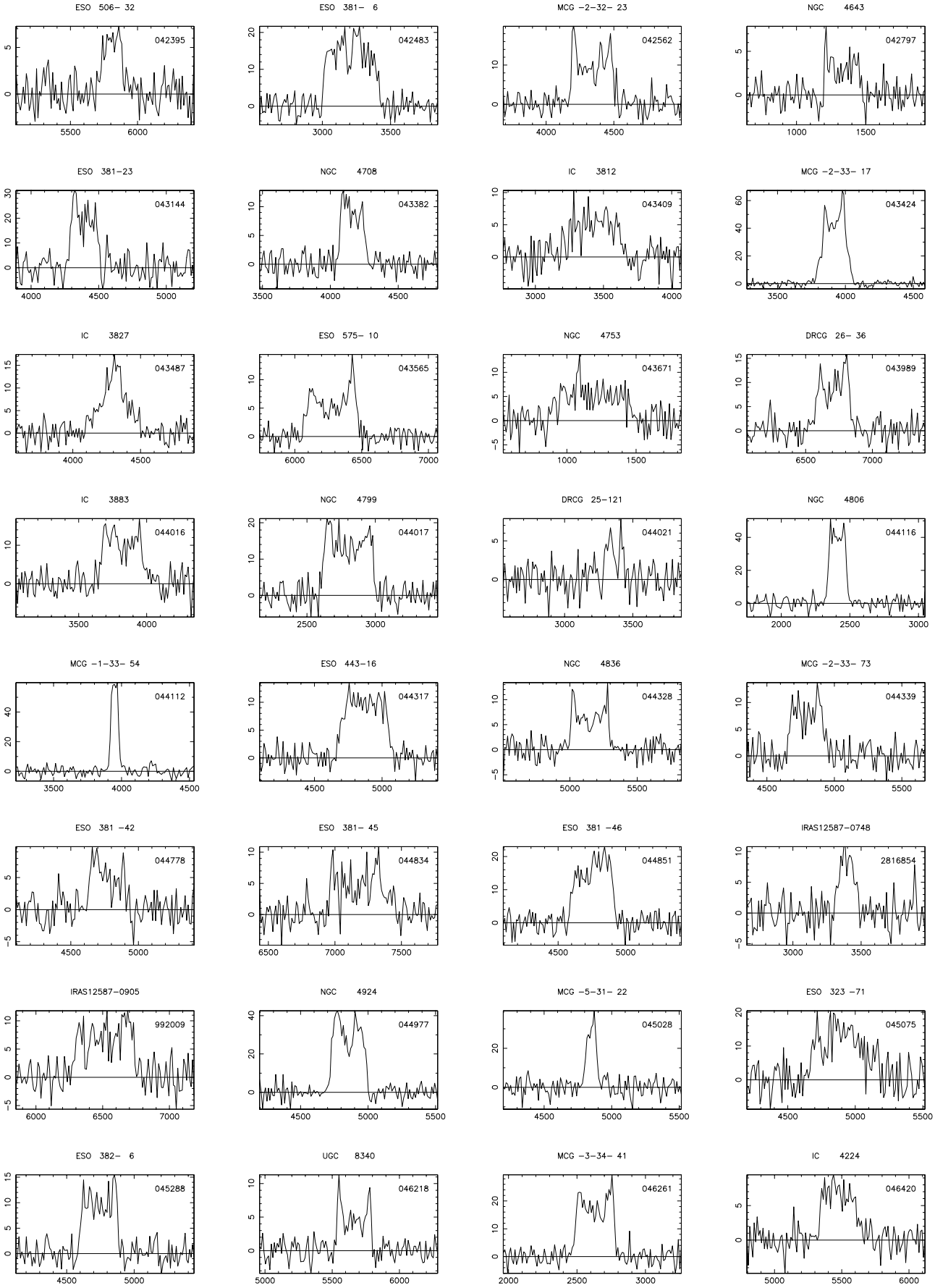

Fig. A.1. continued.

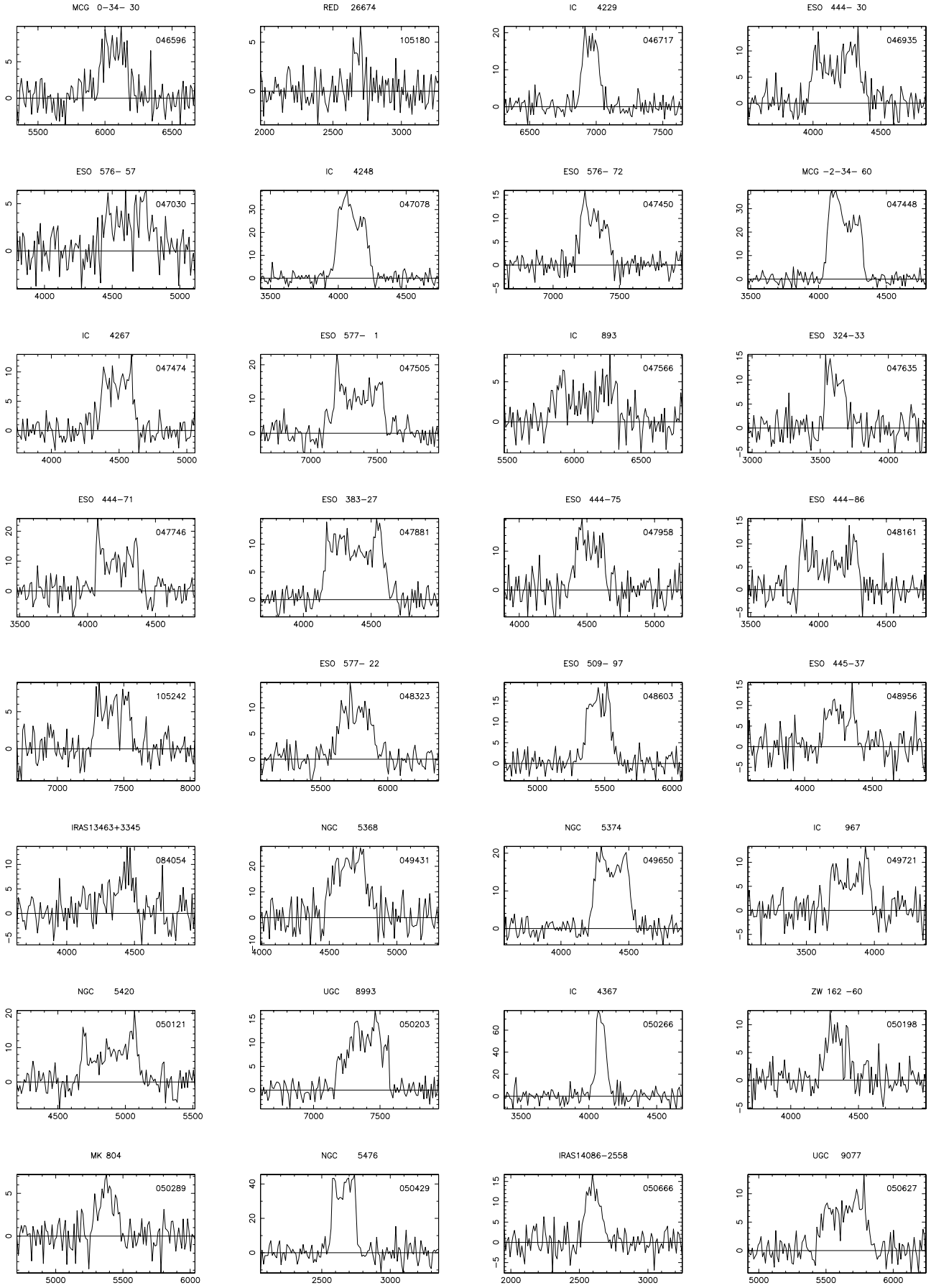

Fig. A.1. continued.

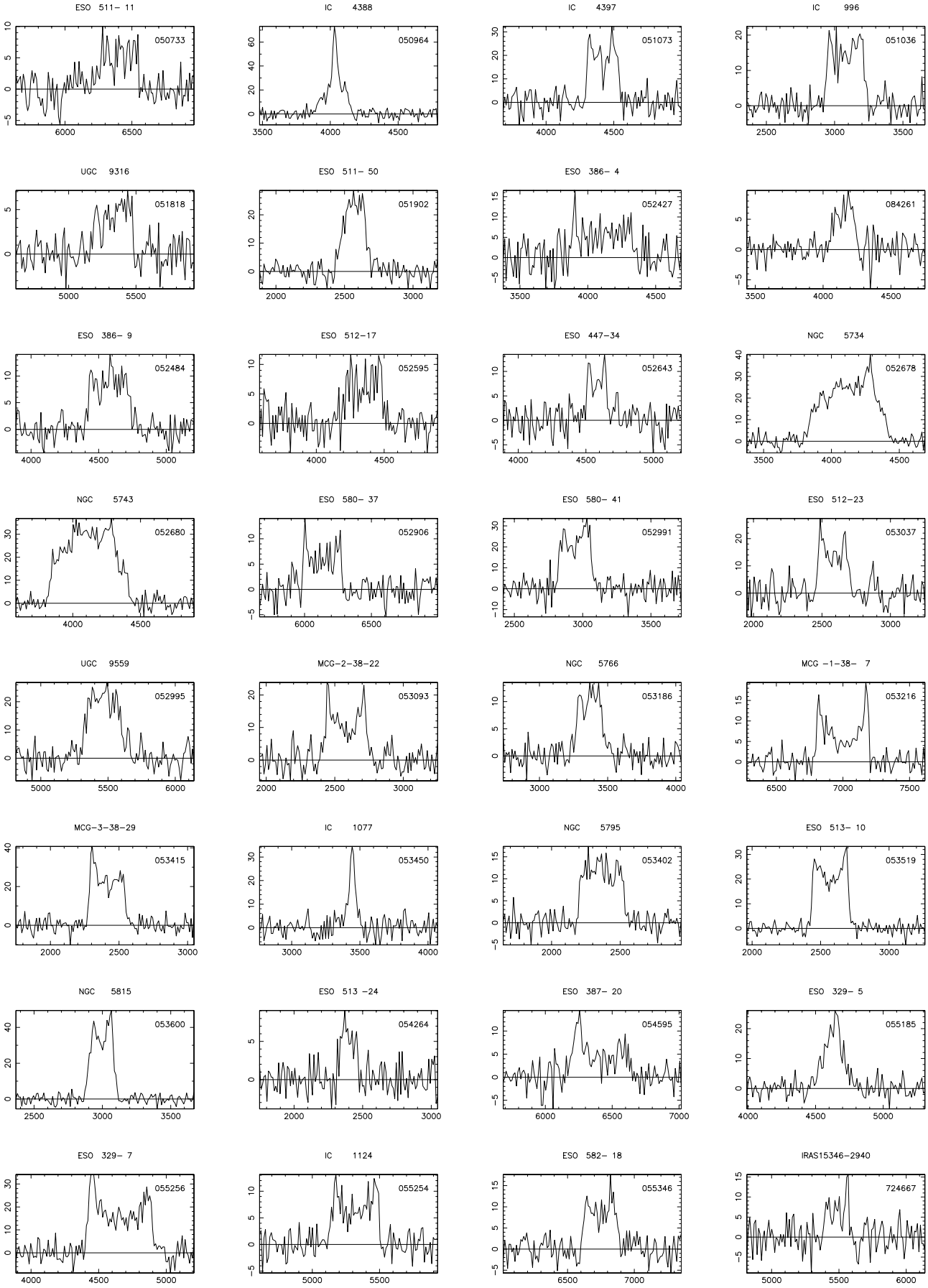

Fig. A.1. continued.

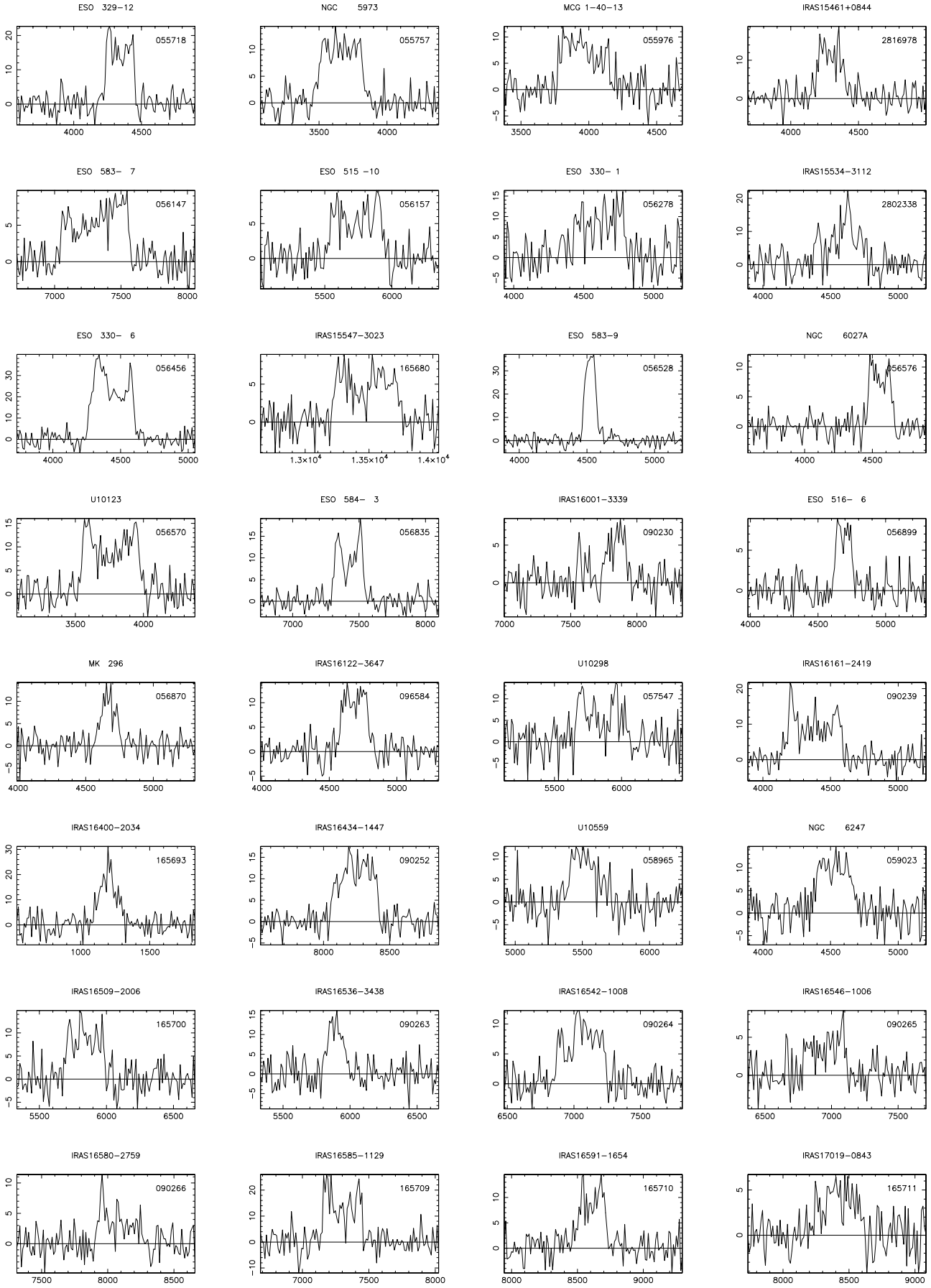

Fig. A.1. continued.

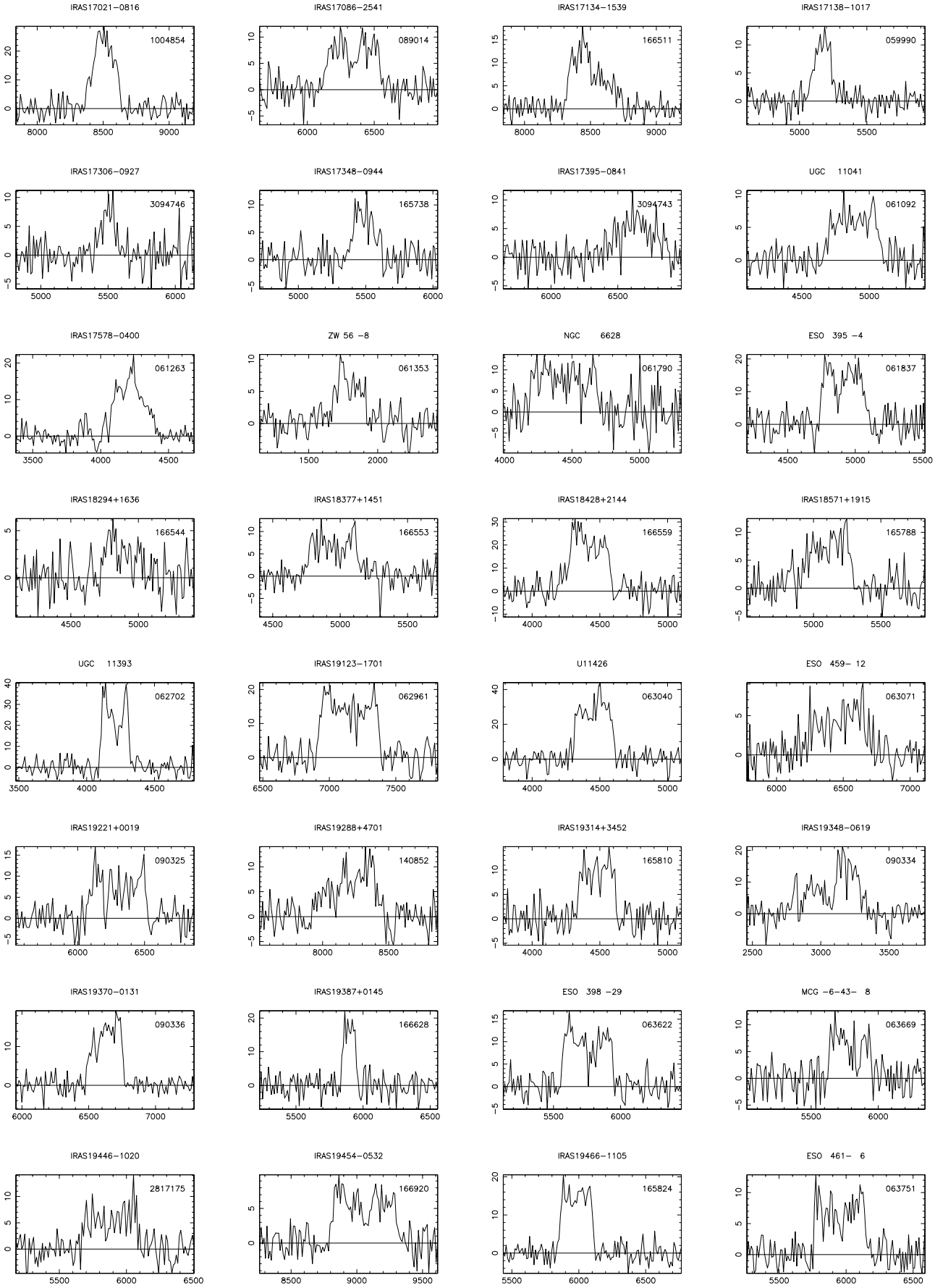

Fig. A.1. continued.

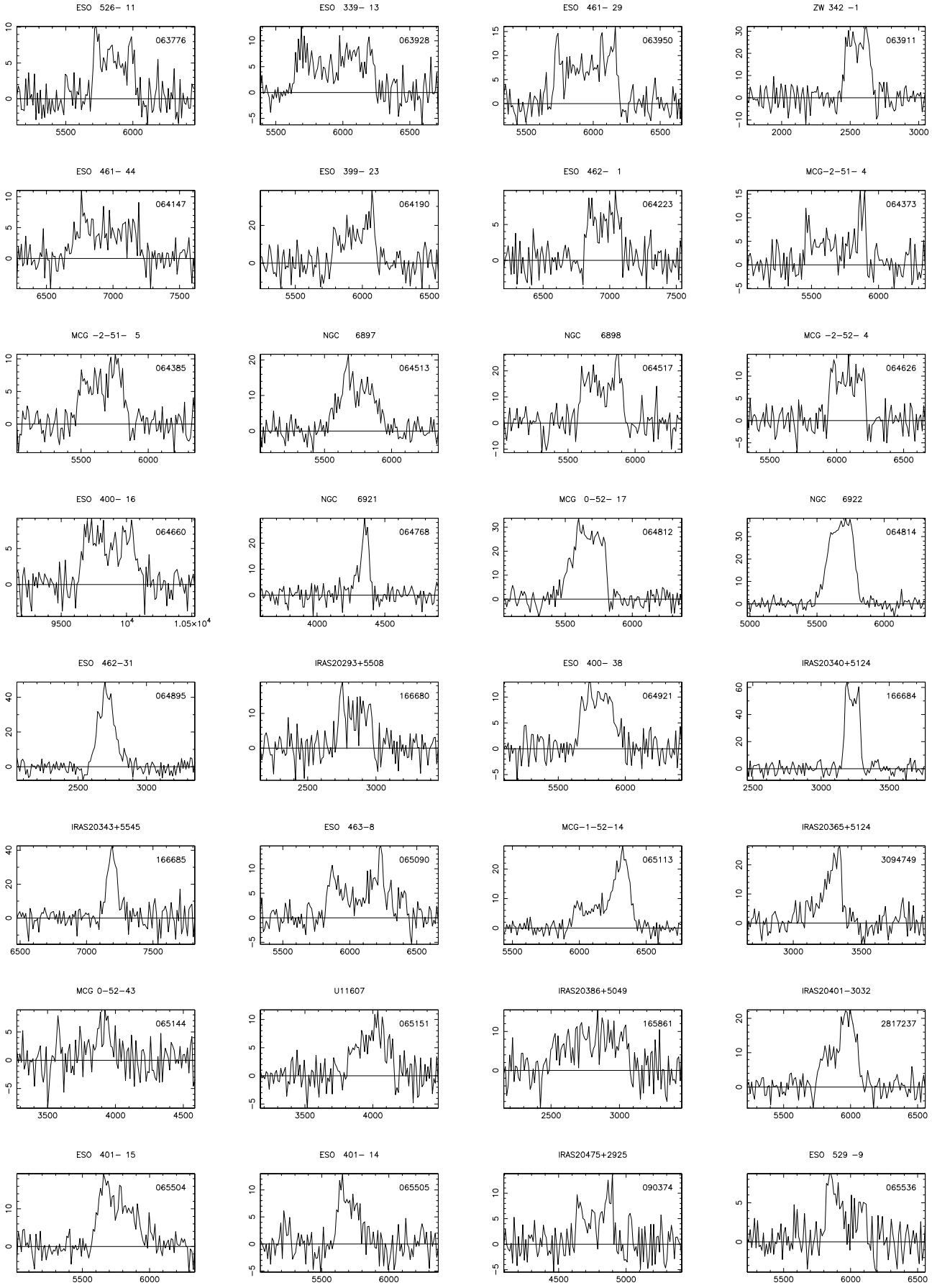

Fig. A.1. continued.

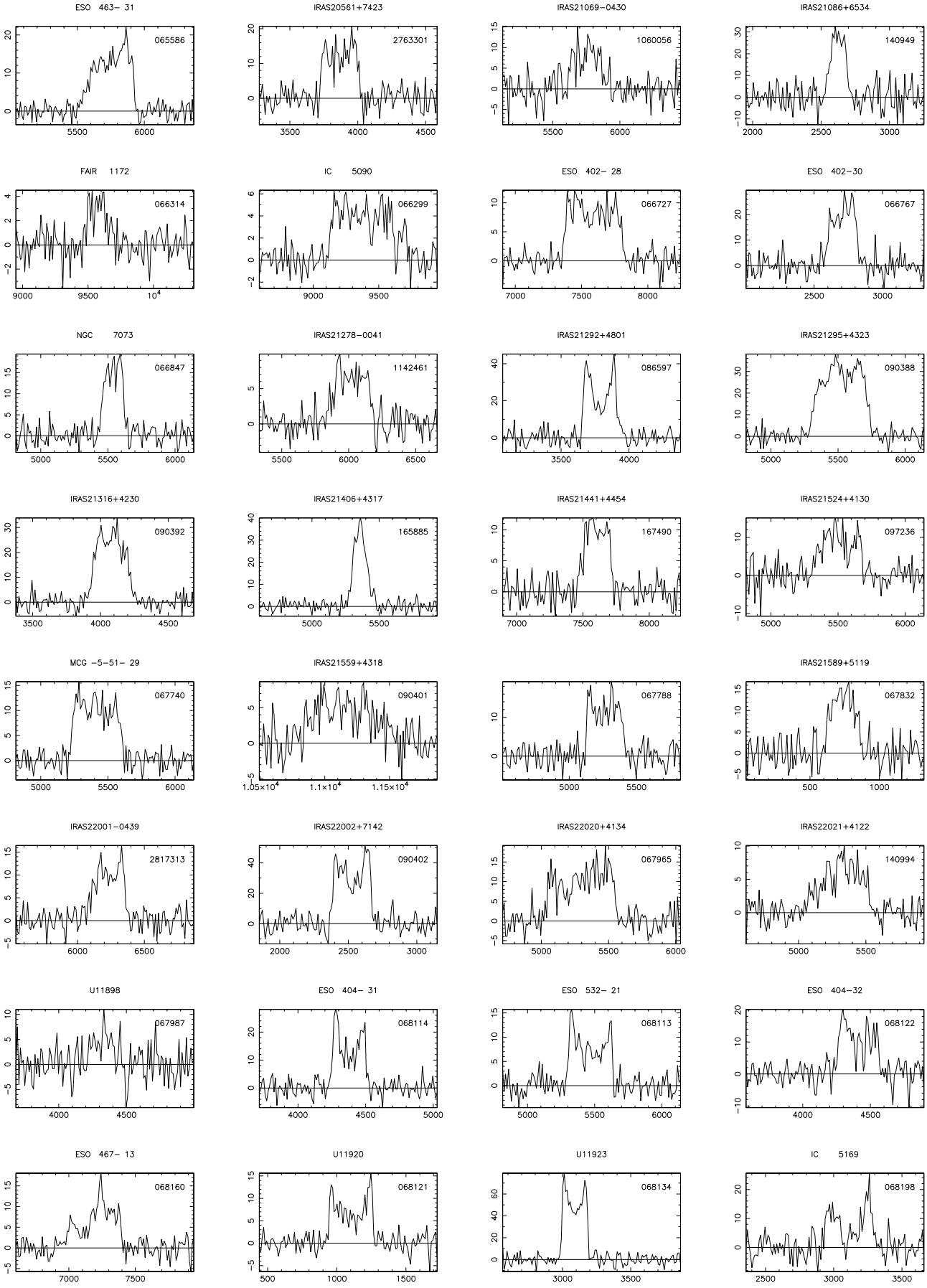

Fig. A.1. continued.

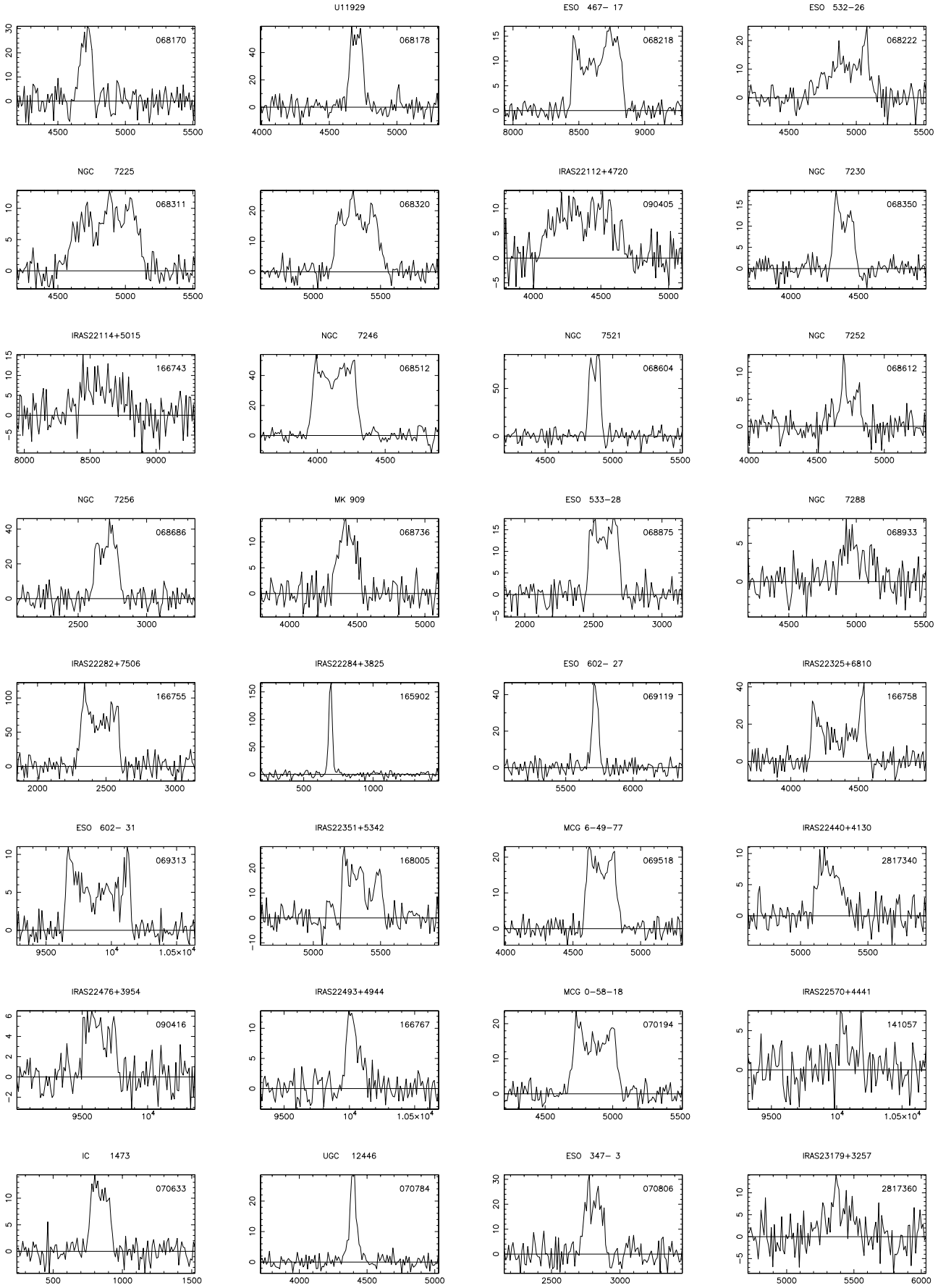

Fig. A.1. continued.

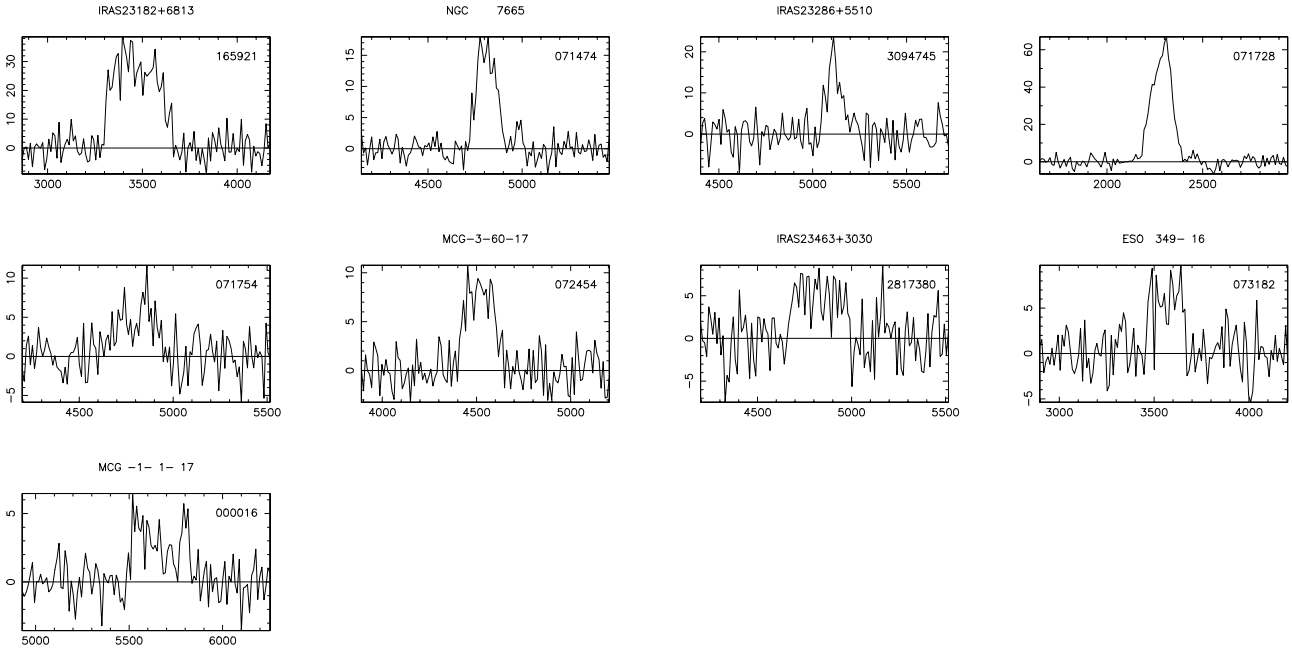

Fig. A.1. continued.